The Role of Radiative Processes in the Diffusional mass Evolution of Cirrus Hydrometeors

By
Douglas Alan Wesley and Stephen K. Cox

Department of Atmospheric Science
Colorado State University
Fort Collins, Colorado

Colorado State University

Department of Atmospheric Science

Paper No. 406

THE ROLE OF RADIATIVE PROCESSES IN THE DIFFUSIONAL MASS EVOLUTION OF CIRRUS HYDROMETEORS

Douglas Alan Wesley

Stephen K. Cox

Atmospheric Science Department

Colorado State University

Fort Collins, Colorado

November, 1986

Atmospheric Science Paper Number 406

ABSTRACT

The mass evolution of hydrometeors in cirrus clouds for various radiative conditions in the cloud and for varying ambient moisture supply is simulated using a time dependent microphysical model. Radiation can play an important role in this mass evolution when only one phase is present. When both liquid droplets and ice crystals are situated in a typical cirroform environment and the moisture supply is limited, radiation produces only a minor effect on the mass evolution of the hydrometeors. In these cases ice crystals grow quickly at the expense of the droplets and the droplets evaporate within several minutes, even under water supersaturation conditions. Radiation does not significantly increase or decrease the survival times of the droplets in the coexisting cases.

In the absence of ice crystals and under certain radiative conditions, the droplets can survive when the environment is subsaturated. For other radiative conditions, the droplets evaporate when the environment is supersaturated. Radiation can also be significant in the mass evolutions of the ice phase alone for suspended crystals.

ACKNOWLEDGEMENTS

This research was supported in part by the National Science Foundation, grant numbers ATM 8209861 and ATM 8521214, and National Aeronautics and Space Administration grant number NAG 1-554. Dr. Graeme Stephens provided advice on several aspects of the model and I also greatly appreciate the help of Steve Ackerman for many consultations on the radiative aspects of the model. Mrs. Judy Sorbie developed excellently drafted figures, and special thanks are due to Ms. Melissa Tucker for patience and preparation of the numerous drafts and final version of the manuscript.

TABLE OF CONTENTS

LIST OF FIGURES

I. INTRODUCTION

Clouds at high levels in the atmosphere (greater than 20,000 feet) present unique problems for the atmospheric scientist. Cirroform clouds blanket large portions of the earth at all times, and thus play a major role in the global radiation budget and climate system. Despite their radiative importance, there has been a historical lack of quantitative studies detailing or modeling the physical processes that create, maintain and dissipate cirrus. One of the most pressing microphysical problems is the composition of cirrus clouds. Due to the extremely cold temperatures associated with cirroform clouds (-20 to -50°C), researchers have concentrated on the ice phase when dealing with cirrus composition. Recent evidence (e.g. Sassen et al. (1985), Curran and Wu (1982) and Griffith et al. (1980)) has indicated that small liquid water droplets may indeed be present in these clouds. Though several studies (e.g. Heymsfield (1975)) report the sizes, habits, and concentrations of typical cirrus ice crystals, lack of reliable liquid water measurement systems on aircraft has left the water phase question unanswered. Theoretical investigations have also dealt with only the ice phase. Knowledge of the exact composition of these clouds is essential in order to quantify the radiative characteristics of the cloud. Such quantification is necessary for any cirrus cloud model and for general circulation models.

Previous studies by Starr and Cox (1985) and Ramaswamy and Detwiler (1985) develop cirroform cloud models, but do not consider the liquid hydrometeor phase. The former investigation finds that radiative processes are very important in the evolution of a cirrostratus cloud layer. The latter concludes that the net radiative cooling rate in the top 5% of the cloud is very sensitive to the crystal sizes and concentrations, as is the net radiative heating rate in the lowest 5% of the cloud. Also, Ramaswamy and

Detwiler show that radiative influences on the growth of ice crystals with lengths less than 200 μm are important only near an ice saturation ratio of unity, and the ambient vapor supply decreases in regions where crystals are growing in a supersaturated environment. Stephens (1983) investigates the effect of radiative transfer on the growth rates of various crystal habits in a cirroform environment, and concludes that radiation acts to enhance (suppress) ice particle growth (evaporation) in a radiatively cooled environment while the reverse applies when radiative heating is present.

The goal of this investigation is to assess the diffusional mass evolution of a population of coexisting crystals and droplets in a cirroform environment including the effects of longwave and shortwave radiation at various locations in the cirrus cloud. First, the mass evolution of droplets and crystals in a one-phase situation are calculated with and without radiative effects for various ambient moisture conditions. Then, coexisting situations are simulated with and without radiation. The model quantifies the effects of a varying ambient moisture supply (simulated updraft/no updraft) and hydrometeor sizes and concentrations on the one-phase and coexisting mass evolutions. Through these simulations, the investigation assesses the possibility of the existence of persistent small water droplets in cirroform clouds, and whether radiation, moisture supply, or particle sizes and concentrations can significantly enhance this possibility.

The microphysical model also simulates the diffusional mass evolutions of ice crystals as they fall from a moist cloud layer to a dry sub-cloud region. The effects of longwave radiation on these growth rates are quantified. These results demonstrate some of the processes involved in the dissipation stage of cirroform clouds.

II. THE MICROPHYSICAL MODEL

In order to realistically assess the detailed radiative- microphysical interactions in cirroform clouds and the possibility of the existence of liquid water layers, one must investigate the thermodynamics/physics of the hydrometeors in a representative upper-level environment. Coexisting simulations refer to droplets and ice crystals situated next to each other in the cloud. The model simulates the diffusional mass evolutions of crystals and droplets of various initial sizes. Also, the model simulates some cases of ice crystals falling through the cloud layer, both with and without longwave radiative effects.

2.1 Individual droplets

For the spherical droplet, the three diffusional growth equations from Stephens (1983) and Rogers (1979) are:

water balance: rate of water gained by deposition = rate of water diffused to droplet

$$dm/dt = 4\pi r D_v' [\rho_v(T) - \rho_{s,w}(T_s)] \quad (1)$$

heat balance: rate of latent heat gained = rate of heat conducted from droplet

$$L_e dm/dt = 4\pi r k_a' (T_s - T) \quad (2)$$

moisture supply: rate of change of saturation ratio = moisture gained from updraft - moisture lost via condensation

$$ds/dt = Q_1 dz/dt - Q_2 d\chi/dt \quad (3)$$

The appendix lists the symbols and their meanings.

The growth equations ignore solution and ventilation effects. Solution effects are negligible for the hydrometeor sizes considered in this study. The assumption of negligible ventilation physically constrains the hydrometeors to move along with the mean wind. This constraint is acceptable for most of the droplet sizes in this study and for relatively small crystals ($L \leq 200\mu m$). Larger crystals are common in convective cirrus uncinus clouds; for a realistic simulation of the mass evolution of these crystals ventilation would have to be considered.

The coefficients of diffusivity (D_v) and thermal conductivity (k_a) are modified to take into account the error involved in treating the microscopic heat and vapor diffusion on the scale of a few microns. The modification of these coefficients is detailed in Pruppacher and Klett (1978) and will not be repeated here.

In equation (3), for each simulation the saturation ratio is prescribed at the initial time and, for the simulated ambient updraft case, is held constant throughout the simulation, and for the coexisting cases (ambient moisture supply is not replenished during hydrometeor growth) the saturation ratio is dictated by the amount of hydrometeor growth or evaporation. Thus, the first term $Q_1 dz/dt$ in equation (3) is not explicitly incorporated into the model equations. The second term has the following form:

$$Q_2 = \rho[R_a T/(\varepsilon e_{sat}) + \varepsilon L_e^2/(pTC_{pa})] \qquad (4)$$

The ambient supersaturation ratio with respect to water plays an important role in the mass evolution of these hydrometeors. This ratio determines the amount of moisture available for the droplet to utilize for growth or evaporation. In the above equations for droplets, the ambient vapor density is defined as:

$$\rho_v(T) = (1+s_w) e_{sat,w}(T)/(R_v T) \qquad (5)$$

where $e_{sat,w}(T)$ is the ambient saturation vapor pressure, and s_w is the prescribed ambient supersaturation with respect to water.

Equations (1) and (2) are solved in an iterative manner for the initial diffusional growth rate of the droplet, assuming an initial size and the ambient conditions discussed in Section 3. The equations are iterated until a T_s is found which satisfies both equations.

In order to simulate a variety of upper-atmosphere situations, five initial droplet sizes were chosen in this investigation to represent the wide range of possibilities of mass evolutions in a cirroform cloud. Each radius was investigated separately. The radii chosen range from a 5 μm droplet to a 200 μm droplet, the latter being about the size of a small drizzle droplet. Further discussion of droplet sizes and concentrations is in Section 3.

2.2 Individual ice crystals

The calculation of the mass evolution of an ice crystal located high in the atmosphere is similar to that of droplets. From Stephens (1983) and Rogers (1979):

$$dm/dt = 4\pi C D_v' [\rho_v(T) - \rho_{s,i}(T_s)] \tag{6}$$

$$L_s dm/dt = 4\pi C k_a' (T_s - T) \tag{7}$$

$$ds/dt = Q_1 dz/dt - Q_2 d\chi/dt \tag{8}$$

Again, symbols are listed and defined in the Appendix. These equations also ignore solution and ventilation effects. In order to calculate the growth rate, some geometry (growth habit) must be assumed. The columnar crystal form is common in regions of cirroform clouds warmer than -40°C [see Heymsfield (1975) and Heymsfield and Platt (1984)]; thus this form was chosen as the crystal growth habit in this investigation. The capacitance C is simply an

effective size parameter. According to Pruppacher/Klett (1978), one may model the shape of a columnar crystal as a prolate spheroid of semi-major and semi-minor axes a and b, for which

$$C = A/\ln[(a+A)/b] \tag{9}$$

$$A = (a-b)^{0.5} \tag{10}$$

(Thus the length of the columnar crystal is 2a while the radius is b). Figure 1 shows a schematic diagram of such a spheroid.

The equations (6) and (7) are solved for the crystal growth rate in the same iterative manner described in section 2.1. The model assumes six initial crystal lengths to best represent the mass evolutions of the entire spectrum of columnar crystals found in a typical cirroform cloud. Each length was investigated separately. These initial crystal lengths range from 10 μm to 400 μm. Further discussion concerning ice crystal habits, sizes, and concentrations is presented in Section 3.

2.3 Radiation and the hydrometeors

Radiation, both infrared (3 to 100 μm) and solar (0.3 to 3 μm) may play an important role in the growth rates of hydrometeors in cirroform clouds. To assess this role, the mass evolutions of crystals and droplets were examined with and without solar radiation, and with infrared radiation values characteristic of three representative locations: cloud base, cloud top, and away from the cloud (the latter being an "isolated hydrometeor" case). The growth equations change to incorporate the effect of infrared and solar radiation. The heat balance equations (2) and (7) contain a new radiative term Q_R which represents the rate of heat delivered to the particle by radiation. For the droplet (following Stephens 1983):

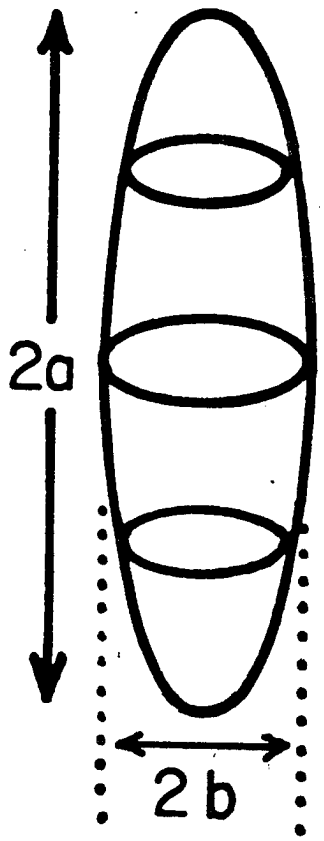

Figure 1. Schematic of a spheroid approximation to a columnar crystal.

$$L_e dm/dt + Q_R = 4\pi r k_a' (T_s - T) \qquad (11)$$

and similarly for the crystal:

$$L_s dm/dt + Q_R = 4\pi C k_a' (T_s - T) \qquad (12)$$

The water and ice balance equations (1) and (6) remain the same for the cases with radiation.

The form of the radiative term Q_R depends on the nature of the radiation and on the particle phase and size. As shown in Stephens (1983) the total radiative power absorbed by a hydrometeor of a characteristic dimension C for radiation intercepted over all solid angles ω is generally

$$Q_R = \int_{\omega}\int_{\lambda} G(C,\omega)\kappa_{abs}(\lambda,C,\omega)[J(T,\lambda,\omega) - B(\lambda,T_s,\omega)]d\omega d\lambda \qquad (13)$$

where: κ_{abs} = particle absorption efficiency

G = geometric cross sectional area of the particle normal to the flow of radiation

J = incident radiation from surrounding environment at source temperature T

B = Planck black body function; emission by the particle at particle surface temperature T_s and wavelength λ.

The absorption efficiency κ_{abs} is also a function of the refractive index of ice or water. In this study, for the computation of κ_{abs} for ice crystals, the model assumes that the particles are spherical for the calculation of the refractive indices. This assumption induces only a very small error in the resulting Q_R as shown by Ramaswamy and Detwiler (1985) and Stephens (1983).

2.3.1 Solar radiation absorption

For shortwave absorption alone by the hydrometeors, the previous equation is simplified since B is negligible and J is simply the solar radiance incident on the particle. Nearly all solar absorption for both ice and water cloud particles is in the near-infrared region, or about 0.7 to 5.0 microns. Also, from Irvine and Pollack (1968), the single-scattering albedo can be approximated with the formula:

$$\omega_\lambda = [1 + \exp(-2k_\lambda r)]/2 \qquad (14)$$

The liquid water absorption coefficient k_λ is a function of the wavelength-dependent complex index of refraction of ice or water. Equation (14) yields an approximation of the particle absorption efficiency:

$$\kappa_{abs} \approx 1-\exp(-2\kappa_\lambda r) \qquad (15)$$

In the shortwave case, the J term in equation (16) takes the form:

$$J(T,\lambda,\omega) = SF_o(\lambda) \qquad (16)$$

where $S = 1376\ W/m^2$ and F_o is a weighting factor which denotes the amount of solar energy in the $\Delta\lambda$ interval. Equation (13) subsequently reduces to:

$$Q_R \approx G(C,\omega)[S \sum_\lambda \kappa_{abs}(\lambda)F_o(\lambda)\Delta\lambda] \qquad (17)$$

where the summation is performed from 0.65 to 5 μm in 0.05 μm increments. The absorption coefficient and the values of F_o were calculated from a Mie theory program obtained from Smith et al. (1980).

2.3.2 Infrared absorption and emission

The magnitude and sign of Q_R for longwave radiation absorption/emission depends strongly on the location of the hydrometeor within the cirroform

cloud. In this investigation, the three chosen locations correspond to: cloud base (maximum longwave warming), cloud top (maximum cooling) and isolated crystal/droplet. In the latter case, the hydrometeor is not located in a cloud; a falling crystal from a glaciated cirrus cloud would fit into this category. These three cases represent limits of longwave radiation net irradiances expected in the cirrus layer.

Between the cloud base and ground surface, a simple approximation is used to simulate the emission/transmission of water vapor, which depends on the ground temperature T_g, the temperature of the atmosphere in this region, and the amount of water vapor and carbon dioxide. The emission/transmission of carbon dioxide in the region below cloud base is much smaller than that of water vapor, so it is ignored in this investigation. Figure 2 shows the flux emissivity as a function of the precipitable water. Using a reasonable estimate of the typical precipitable water (see Section 3) yields an approximation of the emissivity of a clear atmosphere between cloud base and ground. Since this emissivity ε_1 is approximately equal to the absorptance of this layer, the transmissivity is $\tau \approx 1 - \varepsilon_1$. Assuming a transparent atmosphere above the cloud and isothermal conditions within the cloud, the values of $J(T,\lambda,\omega)$ and $B(T_s,\lambda,\omega)$ are: (J becomes the Planck blackbody function for longwave radiation; for a sphere the ω dependence is eliminated)

	$J(T,\lambda,\omega)$	$B(\lambda,T_s,\omega)$
1) cloud base	$\varepsilon_1 B(\lambda,T_{avg})+\tau B(\lambda,T_g)+B(\lambda,T_s)$	$2B(\lambda,T_s)$
2) cloud top	$B(\lambda,T_s)$	$2B(\lambda,T_s)$
3) isolated	$\varepsilon_1 B(\lambda,T_{avg})+\tau B(\lambda,T_g)$	$2B(\lambda,T_s)$

where $T_{avg} = (T + T_g)/2$.

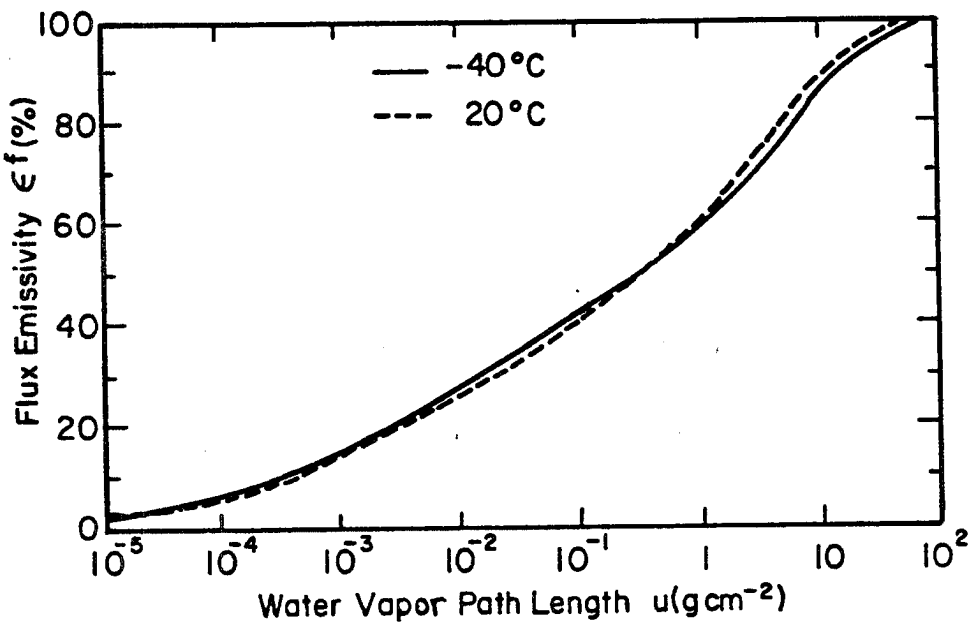

Figure 2. Flux emissivity versus precipitable water for the region below the cloud. (Liou, 1980)

The κ_{abs} values for infrared radiation were obtained from a Mie theory program written by Smith et al. (1980). Thus the general equation for longwave Q_R reduces to

$$Q_R = G(C,\omega) \sum_{\lambda} \kappa_{abs}[J(T,\lambda,\omega)-B(T_s,\lambda,\omega)]\Delta\lambda \qquad (18)$$

where the summation is from 6 to 20 μm in 0.2 μm increments.

2.4 Integration of the growth equations

Assessing the evolution of the hydrometeors in a cirroform cloud requires the calculation of mass evolution over a specified time interval. This requires integration of the growth equations (1), (2), (10), (11), (15), and (16). The integration utilizes the predictor-corrector method of Derrick et al. (1981) which is similar to the method used by Stephens (1983). The predictor equation is the Adams-Bashforth formula:

$$m_{n+1} = m_n+(\Delta t/2)[-(dm/dt)_{n-1}+3(dm/dt)_n] \qquad (19)$$

and the trapezoidal rule is used to correct the value of m_{n+1}:

$$m_{n+1} = m_n+(\Delta t/2)[(dm/dt)_{n+1}+(dm/dt)_n] \qquad (20)$$

Note that at each time step the model uses the iteration procedure described previously to calculate the growth rate. The model utilizes a time step Δt of 5 seconds, and simulates one-hour mass evolutions in each case studied. Some single-phase crystal simulations were run for three hours to investigate the dissipating stage of cirroform clouds. For the variable ice density, Heymsfield (1972) parameterizes the density at -32 °C in cirrostratus as a function of columnar crystal length based on aircraft microphysical measurements:

$$\rho_s = 0.65L^{-0.0915} \qquad (21)$$

where ρ_s is in g/cm^3 and L is in mm. According to Heymsfield, the standard error of estimate for this equation is ± 0.06 g/cm^3.

2.5 Coexisting droplets and crystals

For the previous isolated crystal and droplet cases (both with and without radiation), the ambient moisture supply is held constant throughout the one hour evolution of the hydrometeors, as one might expect in a cloud region with a significant updraft. Such an approach is useful to investigate the relative effects of particle phase, longwave and solar radiation, and moisture supply on the mass evolution of the hydrometeors in a simulated updraft; however, a growing distribution of crystals and/or droplets has an effect on the environmental moisture supply unless this supply is constantly replenished (see Ramaswamy and Detwiler, 1985). In the latter case, the single-phase mass evolutions are simulated with a constant ambient saturation ratio, and the results are discussed in Section 4.

The assumption for the coexisting cases is that no moisture is advected into or out of the cloud volume; i.e., a cumulative mass increase of the hydrometeor population is converted to an equal environmental vapor density decrease for the next time step.

2.6 Simulations of falling ice crystals

This portion of the investigation quantifies the effect of radiation on the diffusional mass evolution of a cirroform ice crystal as it falls from the top of the moist cloud layer through the cloud and into a relatively dry layer. Thus the ambient conditions experienced by the crystal, which determine its growth rate, change as it falls. These conditions include moisture and radiation profiles. As in the previous simulations, ventilation is neglected when calculating the growth rate of the columnar crystals.

To correctly simulate a falling ice crystal, the fall velocity must be calculated. The model utilizes a simple parameterization developed by Heymsfield (1972) based on aircraft microphysical measurements. For columnar cirroform ice crystals in the vicinity of 400 mb:

$$V = AL^B \qquad (22)$$

where the crystal length L is in μm and V is in m/s. The coefficients A and B depend on the length of the crystal as follows:

TABLE 1

COEFFICIENTS FOR FALL VELOCITY PARAMETERIZATION

L (μm)	A	B
0-200	8.114×10^{-5}	1.585
200-400	4.995×10^{-3}	0.807
400-600	2.223×10^{-2}	0.558

The resulting fall velocities range from 0.0010 m/s for L = 5 μm to 0.50 m/s for L = 300 μm.

The crystals fall through a moist 0.5 km-thick cloud layer which is supersaturated with respect to ice. The crystals experience longwave cloud top cooling during the initial period of this fall, radiative equilibrium (Q_R = 0) within the interior of the cloud layer, cloud base warming in the latter portion of the fall near cloud base, and isolated radiative conditions thereafter. Once outside the cloud layer, the atmosphere is subsaturated with respect to ice. Temperature and pressure conditions encountered during the crystal fall are the U.S. Standard Atmosphere sounding. The model time step for the falling crystal cases is one second.

III. SPECIFICATION OF AMBIENT CONDITIONS

This investigation simulates microphysics and radiation in cirrus clouds, so a representative cirroform environment must be specified. Ambient meteorological properties such as temperature, pressure, total ice and/or water content and supersaturation ratio are critical to the determination of the hydrometeor mass evolutions. For radiation calculations, ground temperature and precipitable water below the cloud are necessary prescribed conditions. Crystal and droplet sizes, habits, and concentrations must be chosen to represent the variety of situations often encountered in cirroform clouds.

3.1 Cirrus environment

The environment selected for this investigation is a midlatitude continental fall/winter/spring situation. As stated by Fletcher and Sartor (1951), most cirrus clouds range from 20,000 to 35,000 feet during winter and early spring at 40° latitude over the U.S. This layer corresponds to 6.1 to 10.7 kilometers, which is approximately 460 to 240 mb and -25 to -55°C in the U.S. Standard Atmosphere sounding. Furthermore, cirrus-base temperatures for the same observations typically range from -15 to -55°C. For the present study, to best represent a common cirrus situation in which liquid water could exist, an ambient temperature of -30°C was prescribed. Corresponding pressure in the U.S. Standard Atmosphere sounding is 360 mb at 8.1 km. The model also prescribes a ground surface temperature of +15°C for radiative purposes. Figure 3 illustrates these ambient conditions.

In order to quantify longwave radiative effects on the hydrometeors, the emissivity of the clear atmosphere below the cloud base must be specified. As discussed previously, this emissivity and subsequent transmissivity are functions of the precipitable water in this layer (neglecting a small amount

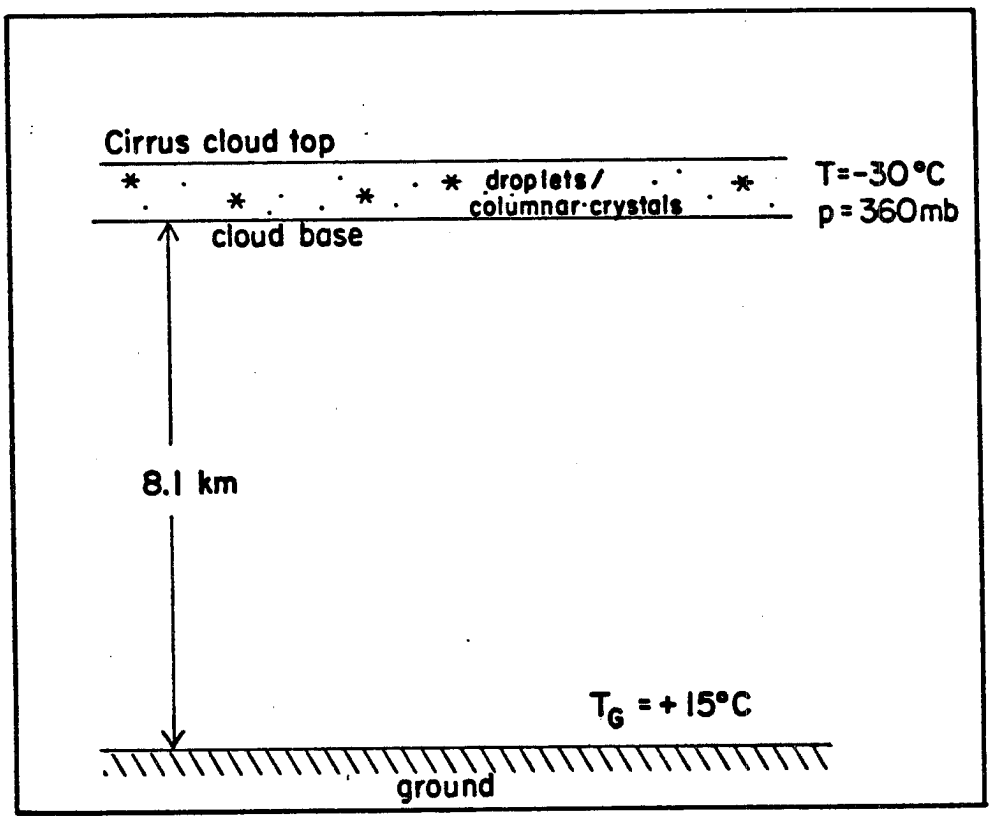

Figure 3. Cirroform cloud environment for this study.

of carbon dioxide absorption and emission). An examination of precipitable water values over Denver for the month of November 1985 yields a range of 0.3 to 1.1 cm.. Thus from Liou (1980) (see Figure 2) the flux emissivity ε_1 is approximately 0.5 to 0.6 and the transmissivity τ is 0.4 to 0.5, with only a weak temperature dependence. In the longwave simulations the model uses ε_1 = 0.55 and τ = 0.45.

3.2 Hydrometeor sizes, habits and concentrations

The model requires an initial size for the hydrometeors. There have been no extensive droplet size measurements made in cirrus clouds, though Curran and Wu (1982) deduced droplet sizes of 3 to 8 μm in upper level clouds. In lower clouds, typical droplet sizes according to Rogers (1979) range from 5 to 100 μm. In order to represent a variety of possible microphysical situations, six initial droplet sizes were chosen for this study: 5, 10, 25, 50, 100 and 200 μm. This spectrum ranges from a small cloud droplet to a small drizzle droplet and encompasses the range of expected possibilities in cirrus clouds.

On the other hand, several detailed microphysical measurements of cirroform ice crystals have been reported. Cirrus crystals can range in size from less than 2 μm to greater than 2000 μm. Sassen et al. (1985) report typical crystal lengths of about 100 μm. Heymsfield (1975) found that only about 5% of crystals observed in cirrostratus clouds were longer than 100 μm. However, the crystals reported in the Heymsfield and Knollenberg (1972) study were often 600 to 900 μm in length. In other actual flights through cirroform clouds, Varley et al. (1978-1979, Parts I-IV) typically found crystal lengths between 5 and 400 μm, with a few larger crystals present. To represent typical microphysical conditions found in cirrus clouds, this model prescribes the following six initial crystal lengths in the simulations:

L = 10, 20, 40, 100, 200 and 400 μm.

Larger crystals are generally scarce in cirrus clouds.

A specification of the total ice or liquid water content (IWC or LWC) along with initial hydrometeor sizes immediately yields the crystal or droplet concentration present for each simulation. IWC and LWC values are commonly reported in cloud microphysical observations. Table 2 lists the various authors and their reported ranges of average ice water contents in various types of cirroform clouds.

TABLE 2

OBSERVED VALUES OF CIRRUS ICE WATER CONTENT

Investigator	IWC (g/m^3)
Sassen et al. (1985)	0.011
Starr (1983)	0.025-0.4
Heymsfield and Platt (1984)	0.001-0.043
Heymsfield and Knollenberg (1972)	0.06-0.15
Heymsfield (1975)	0.01-0.3
Varley et al. (1978-1979)	0.001-0.04

Obviously, a wide range of ice water contents is possible in various regions of cirroform clouds. To represent this range, the following three ice water contents (which determine crystal concentrations) are prescribed for the simulations in this invesigation:

IWC = 0.01, 0.05, and 0.1 g/m^3

Corresponding liquid water contents (if present) of cirrus clouds are not widely known. Sassen et al. (1985) estimates the average LWC of a

upper-tropospheric cloud as 0.06 g/m^3. Lower stratus clouds have typical LWC values of 0.05 to 0.25 g/m^3. Using these approximations, the above values of IWC also serve as an acceptable range for the LWC values used in the simulations.

The resulting droplet and crystal concentration correspond well with reported values for the larger sizes in this study. Heymsfield (1975) reports crystal concentrations of about 0.2 cm^{-3} for cirrostratus clouds, and 0.01cm^{-3} for crystals longer than 100 microns. Other microphysical investigations report cirroform crystal concentrations ranging from 0.01 to 0.5 cm^{-3}, depending on the cloud type. For example, Varley et al. (1978-1979, Parts I-IV) found concentrations from 0.01 up to 2.0 cm^{-3}. The LWC and IWC ranges for this study yield appropriate concentration values for the hydrometeor sizes chosen previously.

In the coexisting situations, some proportion of ice mass to liquid mass must be prescribed, with the total ice plus liquid water contents having appropriate values, as given above. Since no observations of such a proportion are available and since it would probably vary significantly over space and time, the following arbitrary fractions of the ratio of total droplet mass/ crystal mass are prescribed: 0.25, 0.5 and 0.75. By varying this fraction and the concentrations, the simulations will demonstrate the effects of cloud IWC or LWC on the mass evolutions and the effect of the phases on each other.

For the falling crystal simulations, a supersaturation of $s_i = +0.15$ is prescribed in the 0.5 km-thick cloud layer, and $s_i = -0.40$ for the region below the cloud base, which is located at 7.4 km. The cloud top is 7.9 km.

Finally, Table 3 shows the values of Q_R in W/m^2 for the various radiative conditions, first for droplets and then for crystals:

TABLE 3

RADIATIVE TERM Q_R (W/m^2)

Size	Solar	Isolated	Cloud Base	Cloud Top
5	14.8	-18.6	97.9	-116.4
10	29.3	-14.9	121.7	-130.0
25	40.6	-6.8	130.8	-137.6
50	55.8	-4.4	124.8	-129.2
100	74.7	-3.5	118.1	-121.6
200	97.0	-3.0	110.0	-117.2
10	11.2	-7.9	124.1	-61.2
20	14.7	-7.2	133.9	-102.4
40	19.8	-5.3	127.4	-132.0
100	30.1	-4.0	117.5	-139.3
200	37.5	-3.4	112.5	-124.5
400	50.5	-3.0	109.0	-120.5

IV. RESULTS

This Section presents the results of the model simulations in the form of mass evolutions of various hydrometeors in cirroform clouds. Both single-phase, coexisting and falling ice crystal cases with varying radiative conditions are discussed. Radiative, moisture, size and concentration variables can have important influences on the mass evolutions.

4.1 Mass evolution of single-phase hydrometeors

For droplet and ice crystal mass evolutions the model compares well with the results of other researchers. Figure 4 shows a single-phase crystal mass evolution (no radiation) at 690 mb, -9°C, and zero supersaturation (with respect to water; this corresponds to about 10% supersaturation with respect to ice) with initial columnar crystal length of 15 μm. The two results are very similar; the slight difference in masses after 400 seconds is probably a result of the mass integration procedure used by Pruppacher and Klett, which was not specified.

The results of Roach (1976) also allow a comparison of single-phase mass evolutions of droplets including radiative effects. Figure 5 illustrates the mass evolution of individual droplets with $Q_R = -30$ W/m² (Roach's maximum cooling radiative condition). The slight effect of the solute is seen in the early stages as a slightly higher growth rate for Roach. Overall these curves are nearly identical for this radiative cooling case.

The radiative effect on the mass evolutions of crystals or droplets alone depends on the location of the hydrometeor with respect to the cloud and the nature of the radiation (solar or longwave). For droplets at constant saturation with respect to water, radiation can induce significant growth or evaporation (see Figure 6). In this case the droplet has an initial radius of 100 μm. Over the hour of simulation, the cloud top case induces growth to

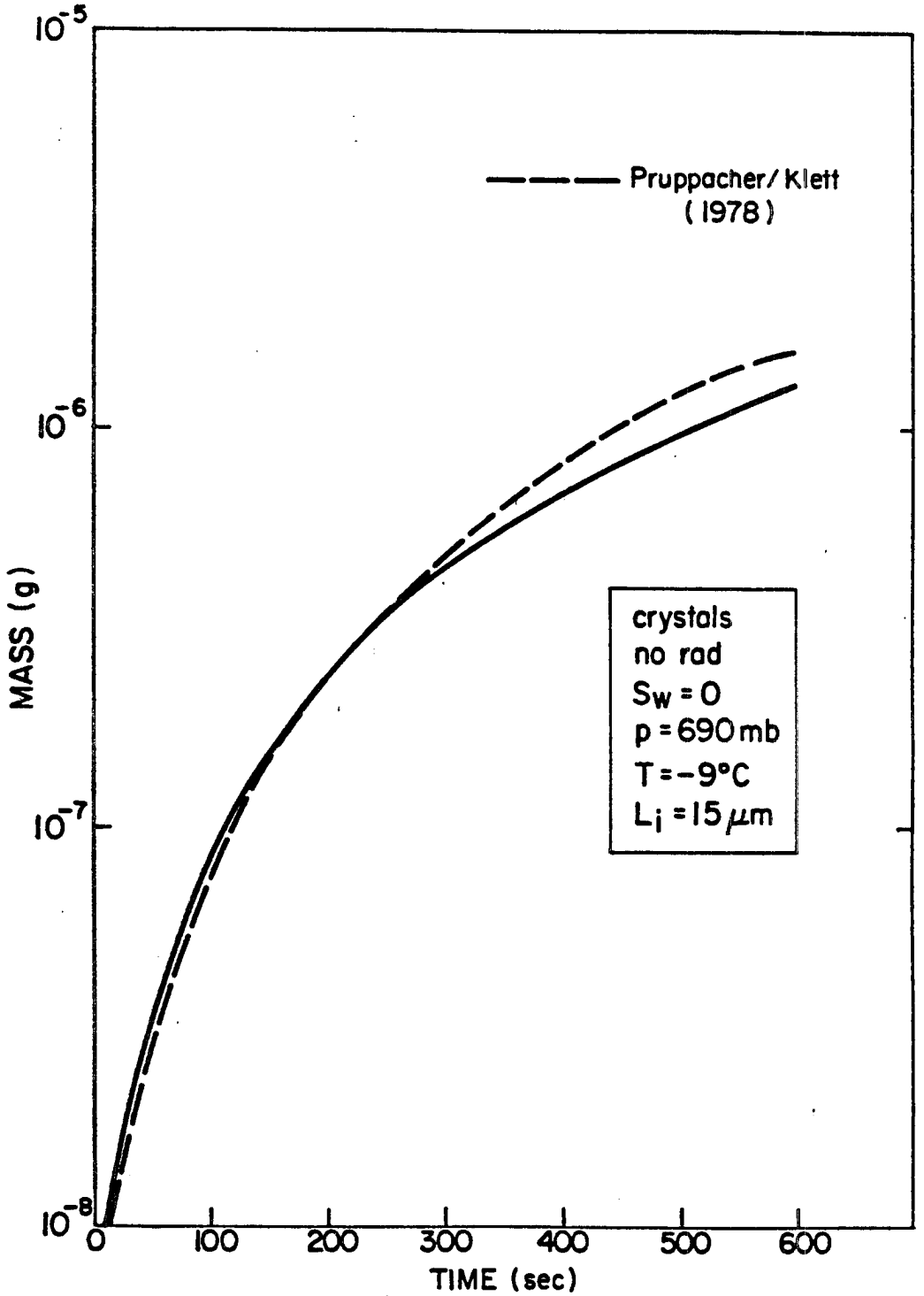

Figure 4. Mass evolution of crystal for two investigations; no radiation.

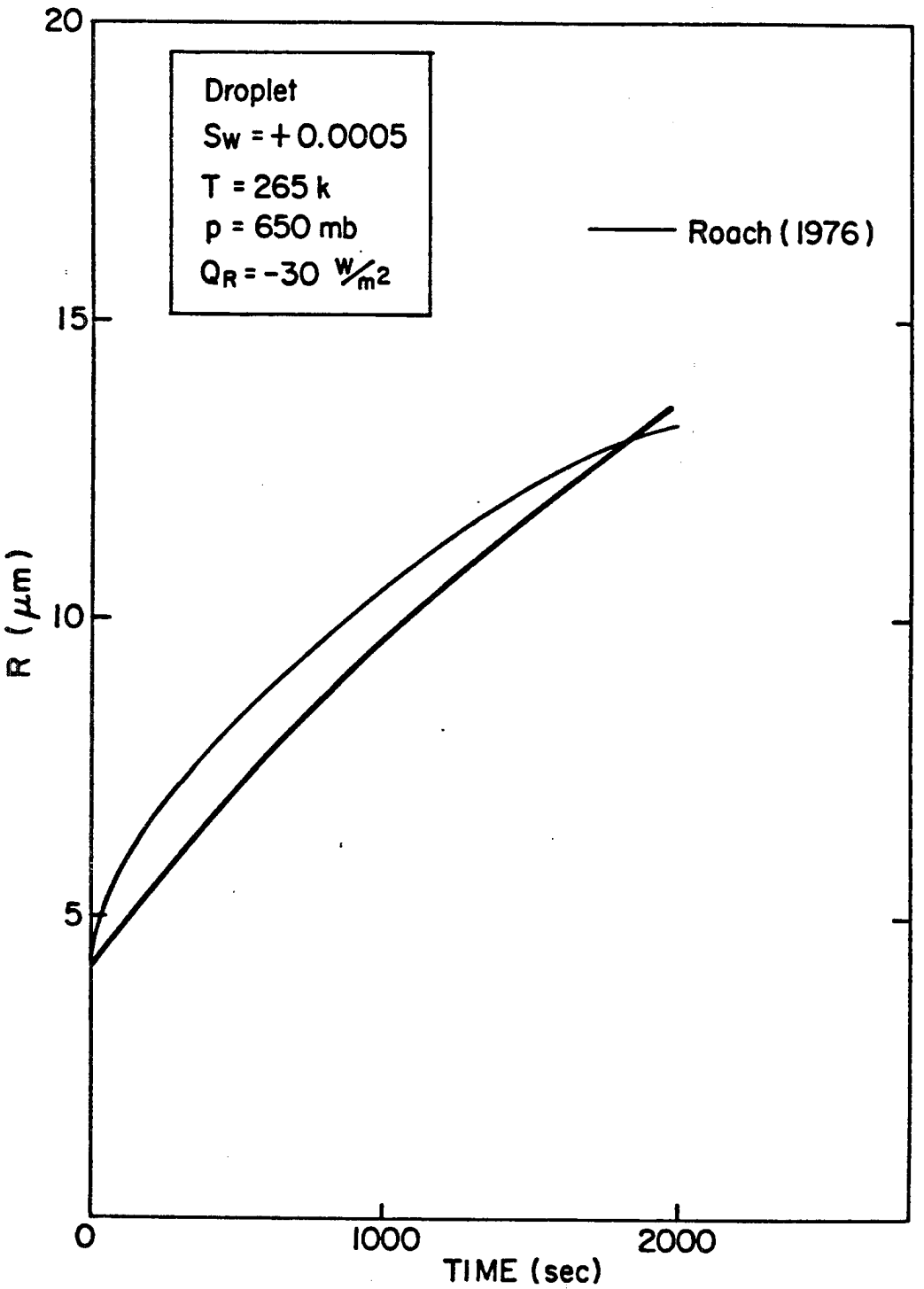

Figure 5. Diffusional mass evolution of droplet for two investigations; no radiation; with radiative cooling.

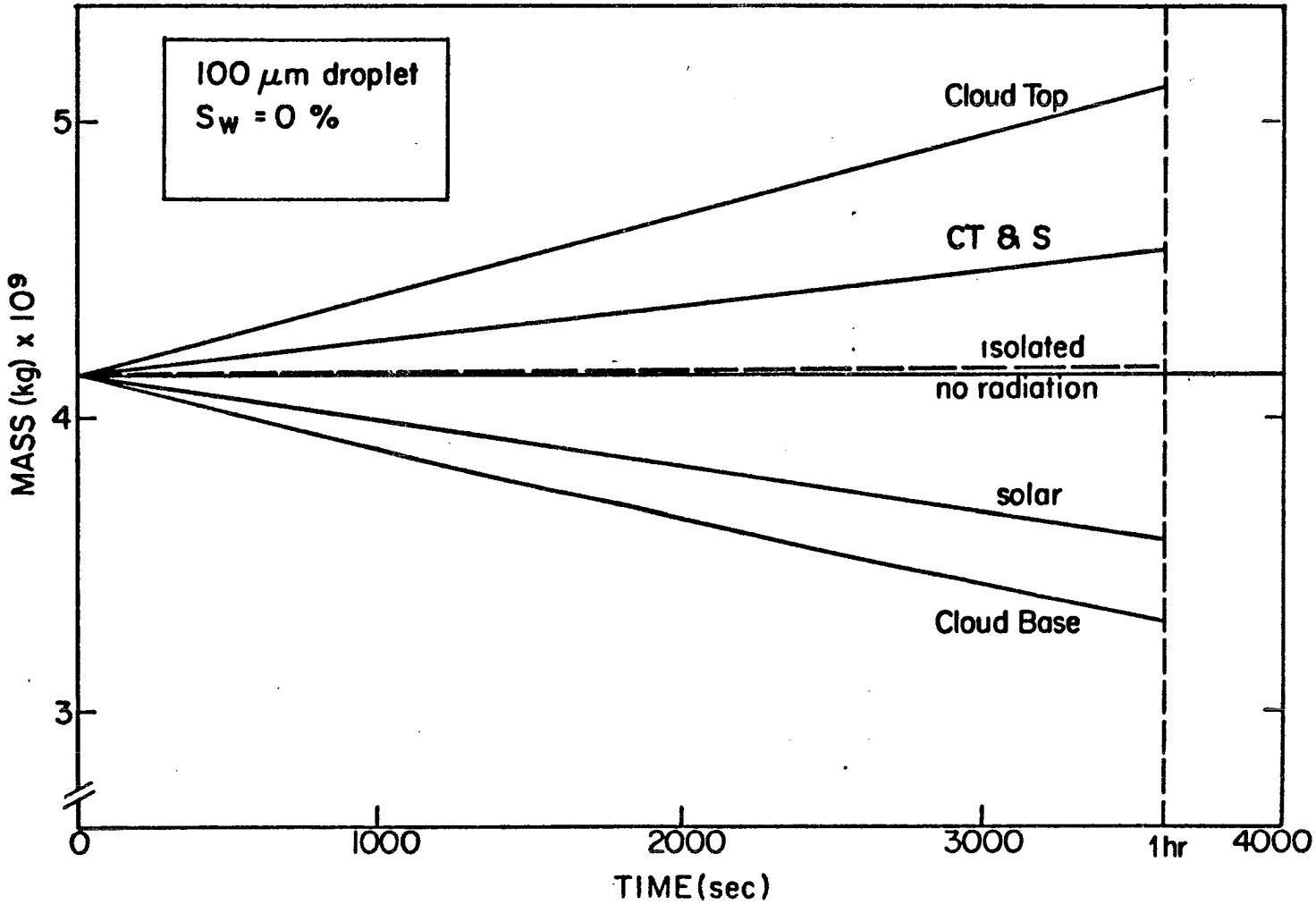

Figure 6. Radiative effect on initial 100 μm droplet mass evolution. (CT&S refers to daytime cloud top case)

about 107 μm, and in the cloud base case the final radius is about 92 μm. The isolated case has little effect on the mass, while the shortwave case induces slight evaporation to about 95 μm. Results from subsequent isolated cases will not be shown on any graphs since the radiative effect is negligible (see the small values of Q_R in column 2 of Table 3). For hydrometeors experiencing isolated longwave conditions at night in a cirroform environment, the net radiation term Q_R is near zero and the crystal or droplet is nearly in radiative equilibrium.

As shown in Figure 6, in a cloud at night the overall effect is to increase the droplet size at the top of the cloud and to decrease the size at the cloud base. Such a situation would tend to reduce the depth of a simulated cirroform cloud due to the relative fall speeds of the growing and evaporating droplets.

Figure 7 represents another single-phase droplet case, but at a constant 1% supersaturation with initial radius 5μm. In this case droplet growth is present in all of the radiative situations. The droplet grows to about 35 μm at cloud top after 1 hour as a maximum, and to about 26 μm at cloud base as a minimum. Also shown is the no radiation case for the droplet with constrained moisture supply and 0.01 g/m^3 initial water content (droplet concentration is 60.8 cm^{-3}), where growth is significantly reduced to only 17.6 μm. Here the environmental vapor density is recalculated at each time step according to the change in droplet mass since the last time step (see Section 2.5). The latter case indicates that once the hydrometeor loses its ambient moisture supply (i.e. becomes separated from the simulated updraft), the potential for further growth is reduced greatly.

Another single-phase hydrometeor situation is shown in Figure 8. These curves illustrate two single-phase mass evolutions: the 200 μm droplet (case

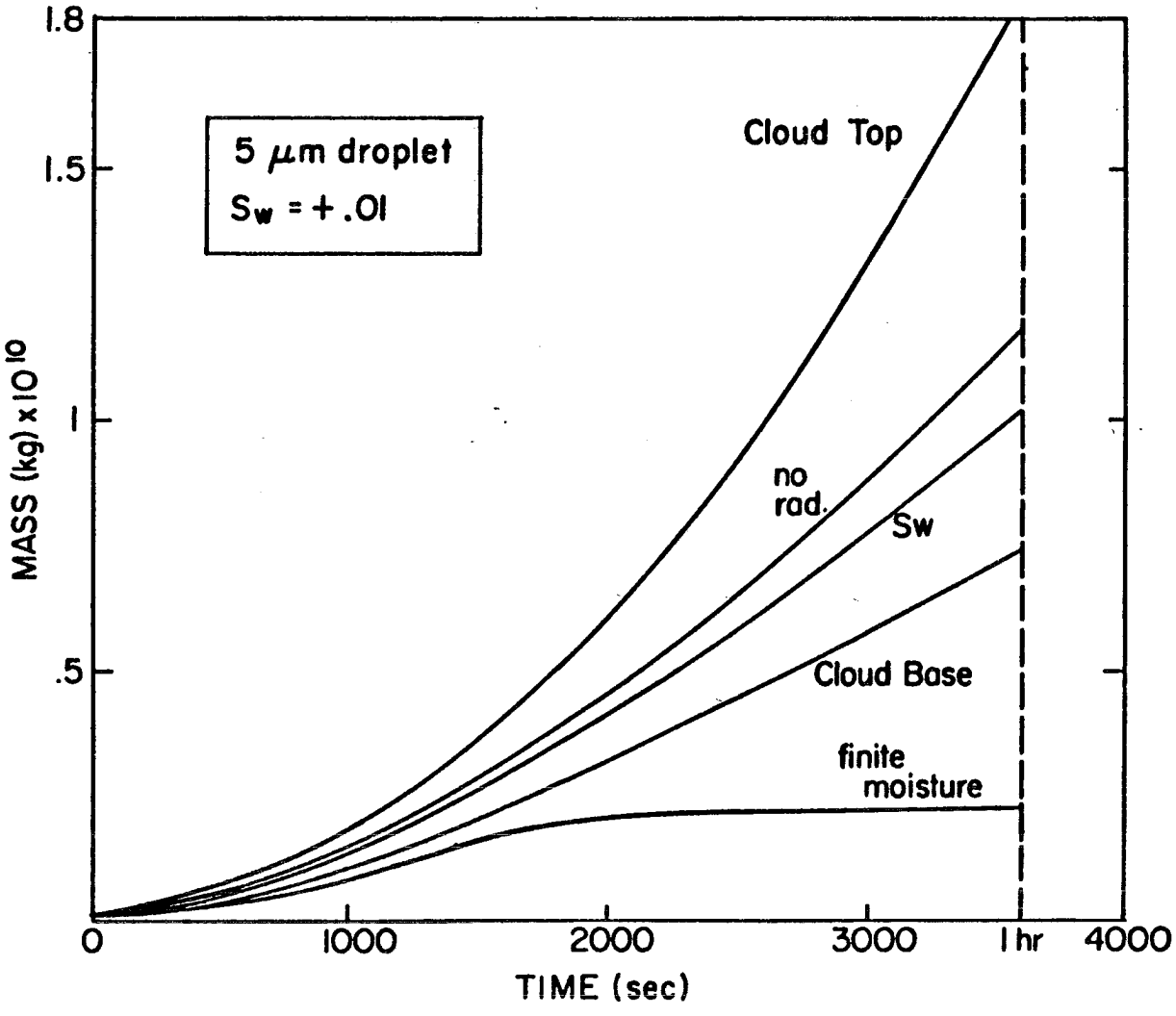

Figure 7. Radiative effect on initial 5 μm droplet mass evolution.

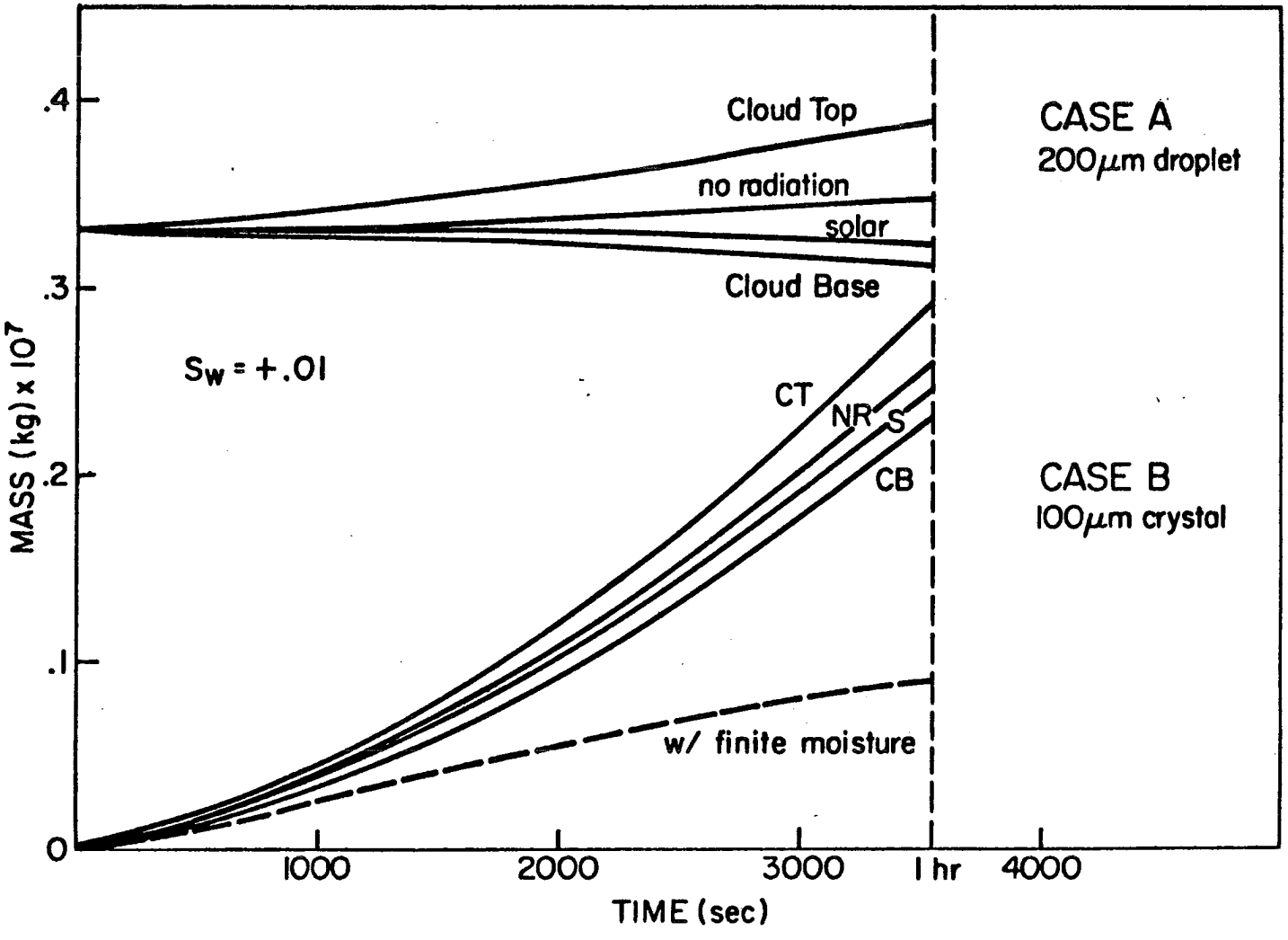

Figure 8. Two single-phase mass evolutions, with and without radiation.

A) and the 100 μm ice crystal (case B). The effect of radiation on individual crystals is similar qualitatively but larger quantitatively than that on droplets. However, in all ice crystal simulations with s_w = -15, -5, -1, 0, +1, and +2%, the environment is sufficiently supersaturated with respect to ice to cause crystal growth, regardless of the radiative conditions. As shown in Figure 8, longwave cooling at cloud top induces additional crystal and droplet growth compared to the no radiation case, while solar and cloud base radiative conditions induce slightly slower growth. In the isolated crystal case, the effect of radiation on the mass evolution is negligible so again this condition is not shown.

The dashed line in Figure 8 represents the mass evolution of the 100 μm crystal with a constrained moisture supply. Here, the crystal concentration is 0.013 cm^{-3}. Outside the simulated updraft the crystal growth is drastically reduced since the initial +35% supersaturation with respect to ice steadily decreases to +2% after one hour. Final crystal lengths are approximately 650 μm for the constant s_i case (no radiation) and only 450 μm for the changing s_i case.

In Figure 9 two more individual mass evolutions are shown. The ambient supersaturation ratio with respect to water is a constant -5% (+27.1% with respect to ice) and the hydrometeor masses are initially about the same. Within 10 to 15 minutes, regardless of radiation, the initial sized 200 μm crystal has surpassed the 100 μm droplet in mass. During the early stages of the mass evolutions, the magnitude of the effect of radiation is approximately equal for both the droplet and the crystal. Therefore the point at which the droplet and crystal are exactly equal in mass does not vary significantly with the magnitude of Q_R, the radiation term in the growth equations. Even in a simulated updraft case for the cirroform cloud (as shown in Figure 9),

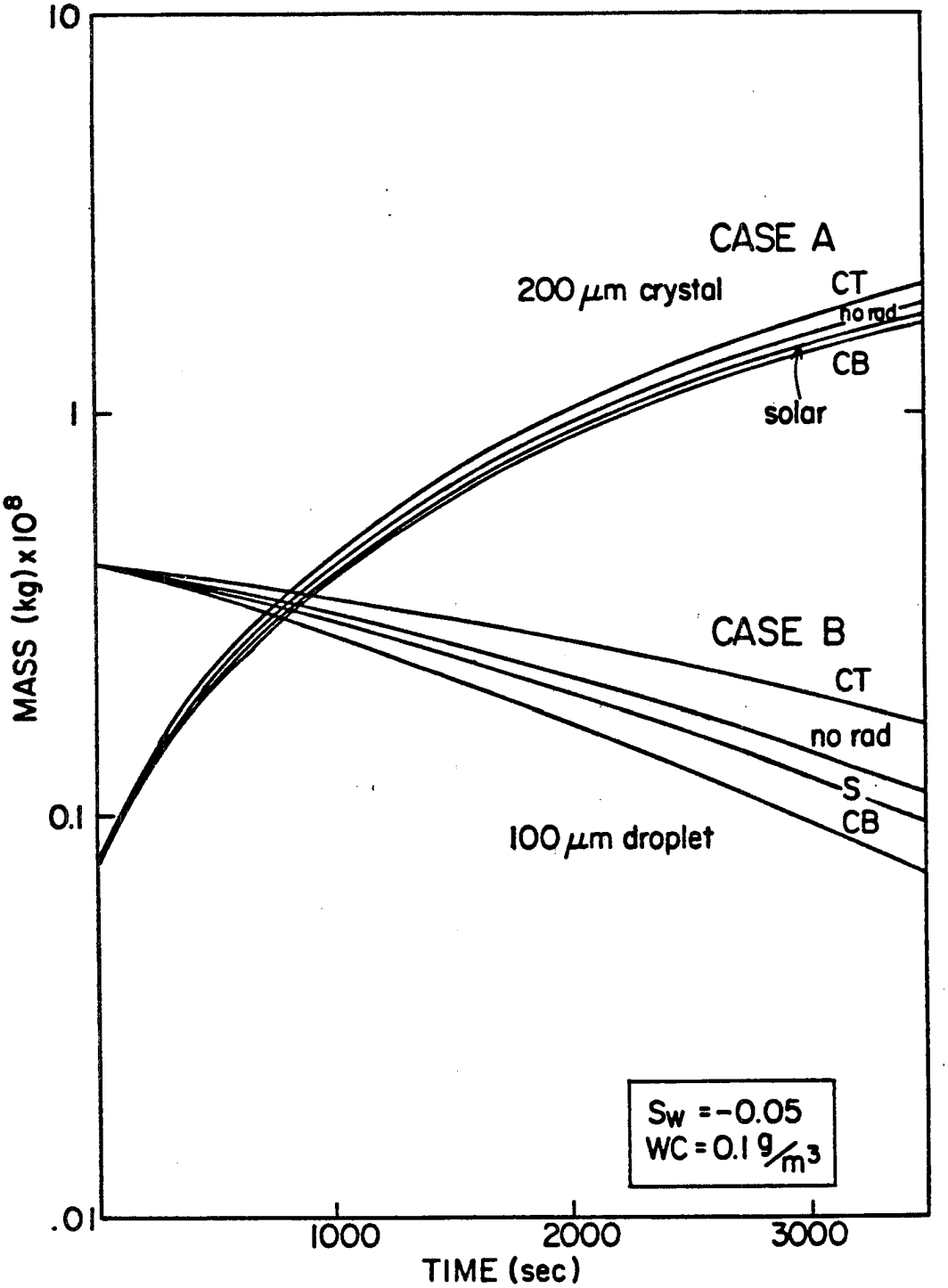

Figure 9. Two single-phase mass evolutions, with and without radiation.

crystals reach much larger sizes than droplets on time scales of one hour. Thus from diffusional growth arguments alone, a situation in cirrus where droplets and crystals of about the same mass coexist in a weak simulated updraft is transient (unless nucleation of new crystals or droplets is taking place).

In actual cirroform clouds, one is likely to encounter situations where the ambient saturation ratio is close to ice saturation and far below water saturation (-25 to -30% supersaturation ratio). In these cases the lifetimes of droplets would be very short, but the effect of radiation on the growth of ice phase is important. The simulation shown in Figure 10 for a crystal of 200 μm initial length demonstrates that cloud-top cooling is large enough to induce crystal growth at $s_i = -0.01$. Final crystal lengths after one hour are about 140 μm at cloud base, 160 μm for solar, 170 μm for no radiation, and 207 μm at cloud top.

Figures 11 and 12 demonstrate the dramatic effect of ambient moisture supply on the mass evolutions of the 10 and 200 μm crystals, respectively, for three hours of simulation and for $s_i = -0.05$, 0.0, and +0.05. For both initial sizes, the lifetimes of the $s_i = -0.05$ cases are short (30 seconds for $L_i = 10$ μm; about 45 minutes for $L_i = 200$ μm), while the +0.05 cases show rapid growth. Radiation is significant except for the 10 μm, $s_w = \pm 0.05$ simulation; for the $s_i = 0.0$ and $L_i = 10$ μm case cloud base warming induces evaporation in about three hours. Cloud-top cooling, on the other hand, quadruples the crystal length in three hours. Overall, for the smaller crystal, radiation is not very significant unless the supersaturation term is very close to 0, and this result is in good agreement with that of Ramaswamy and Detwiler (1985). Radiation plays a major role for the larger crystal in all three cases of $s_i = -0.05$, 0.0, and +0.05.

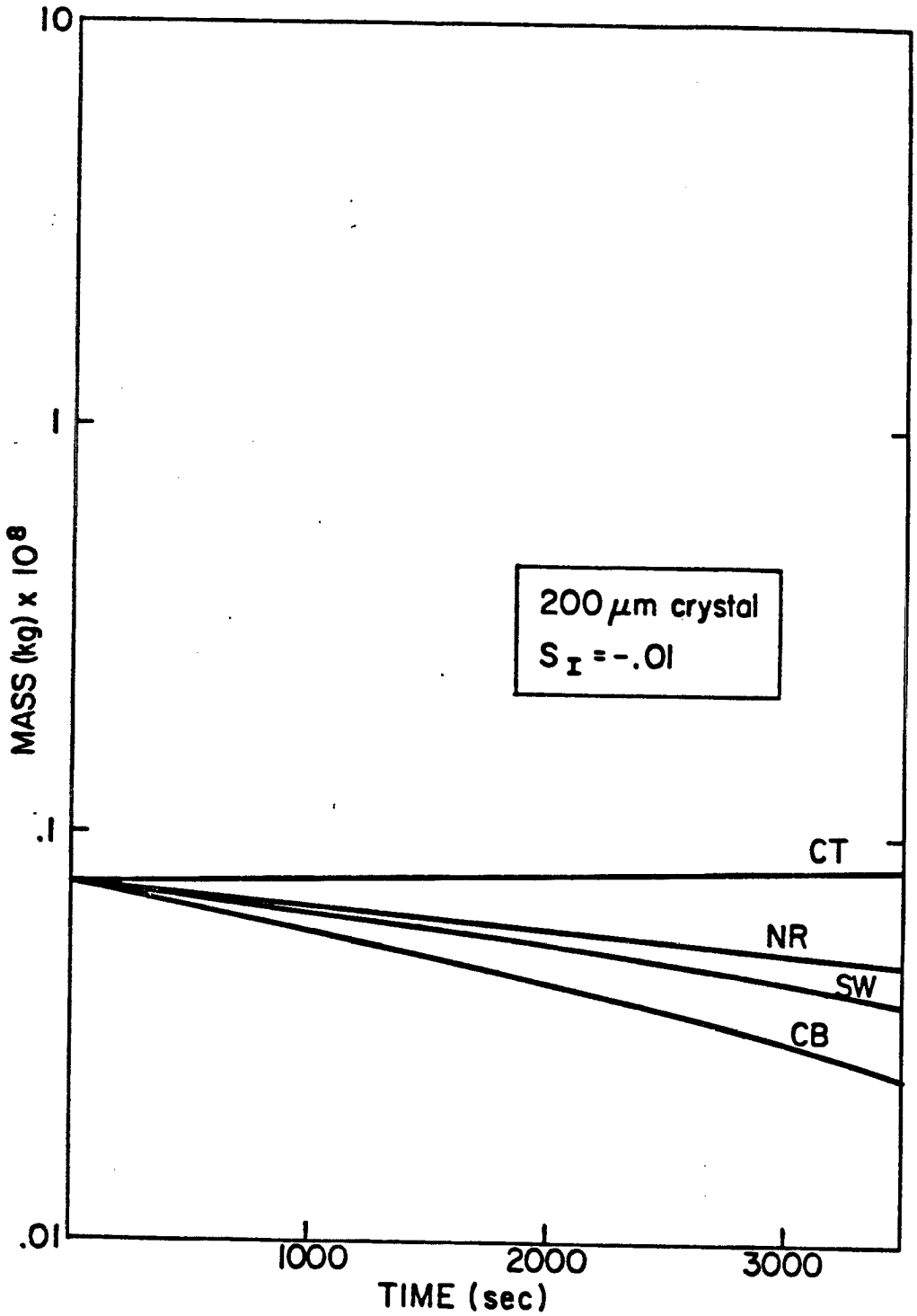

Figure 10. Single-phase crystal mass evolution.

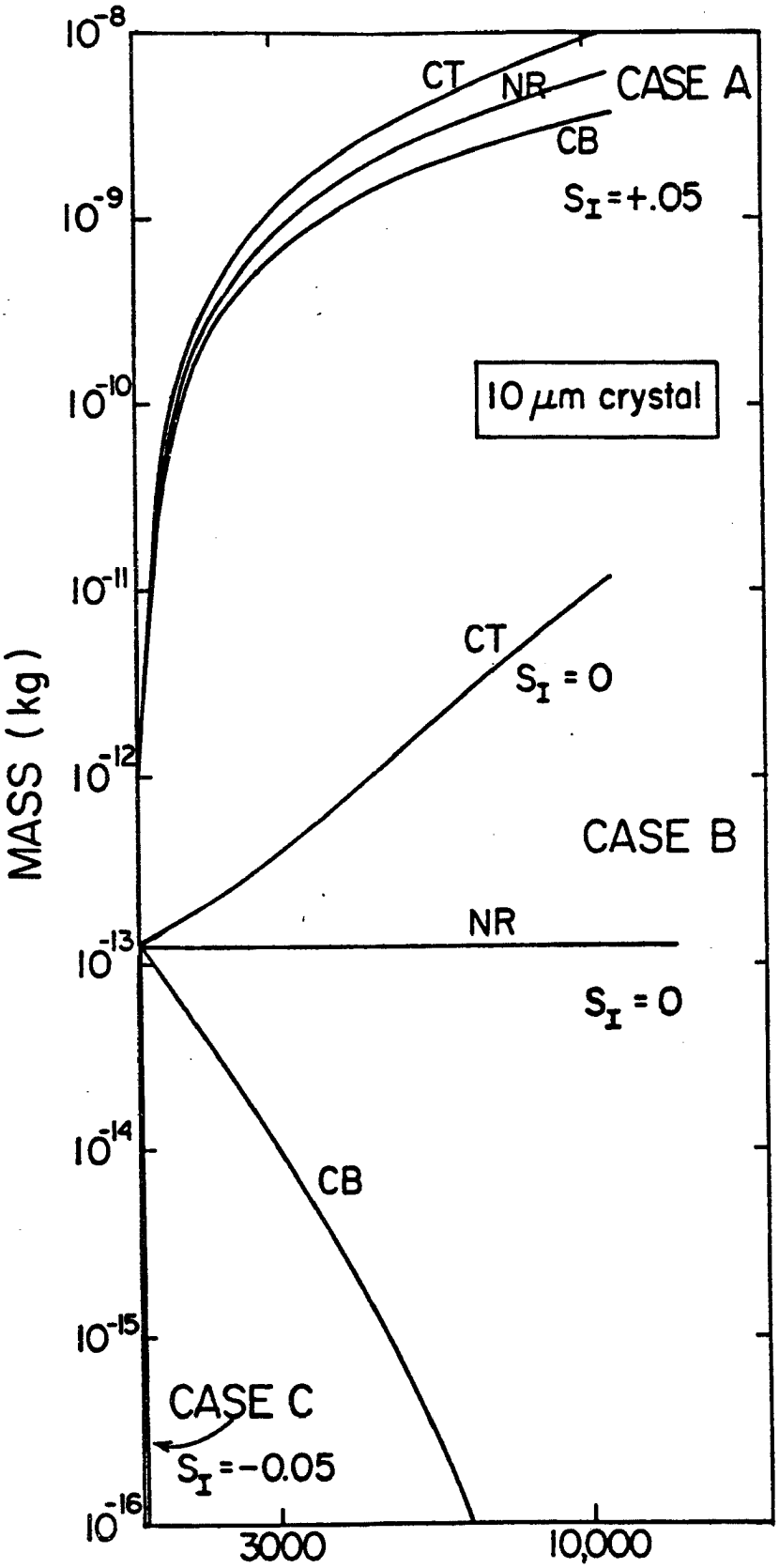

Figure 11. Single-phase crystal evolutions at three environmental saturation ratio values.

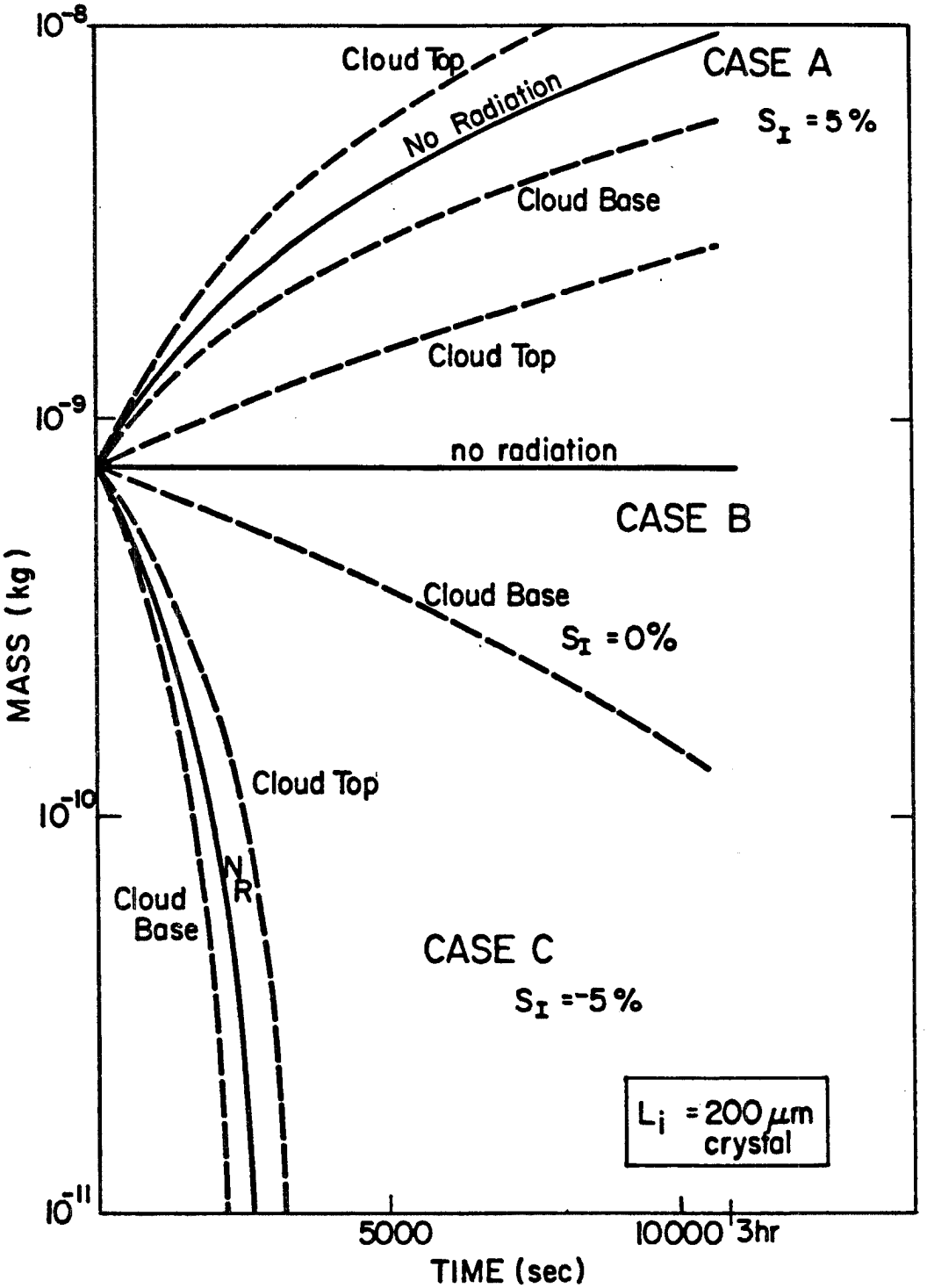

Figure 12. Single-phase crystal evolutions at three environmental saturation ratio values.

4.2 Mass evolution of coexisting droplets and crystals

The assessment of the possibility of liquid water in cirroform clouds concerns the coexistence of ice crystals and water droplets more than the single-phase simulations. The model treatment of the change in ambient moisture for the coexisting simulations is discussed in Section 2.5. In cirrus clouds, significant updraft regions (e.g. in generator regions of cirrus uncinus) do not comprise the majority of cloud volume. Most cirroform cloudiness exists in regions of weaker vertical motion; the coexisting simulations of this investigation apply to these regions. Obviously, a population of growing or evaporating hydrometeors of any significant size can have a marked effect on the ambient saturation ratio in these regions, which then in turn directly affects the subsequent hydrometeor mass evolution. The simulations here assume no new moisture is advected in or out of the cloud region, so they represent the maximum effect of the hydrometeors on the environmental moisture.

Two coexisting simulations, shown in Figure 13, demonstrate some significant results of this initially supersaturated situation. Here 100 μm droplets are situated with 200 μm ice crystals (case A). The initial liquid plus ice water content of 0.1 g/m^3 is composed of 75% liquid (in the form of droplets). Although the initial 100 μm droplets have a much larger mass than the 200 μm columnar crystals, and though the environment initially is 2% supersaturated with respect to water, within the first five minutes the droplets begin to evaporate; the crystals grow quickly throughout the simulation. This is characteristic of all the coexisting simulations. The droplet evaporation rate increases with time as the crystals grow, until the droplets evaporate completely (after about 40 minutes in this case). Figure 13 also shows a coexisting simulation with 50 μm droplets and 100 μm crystals

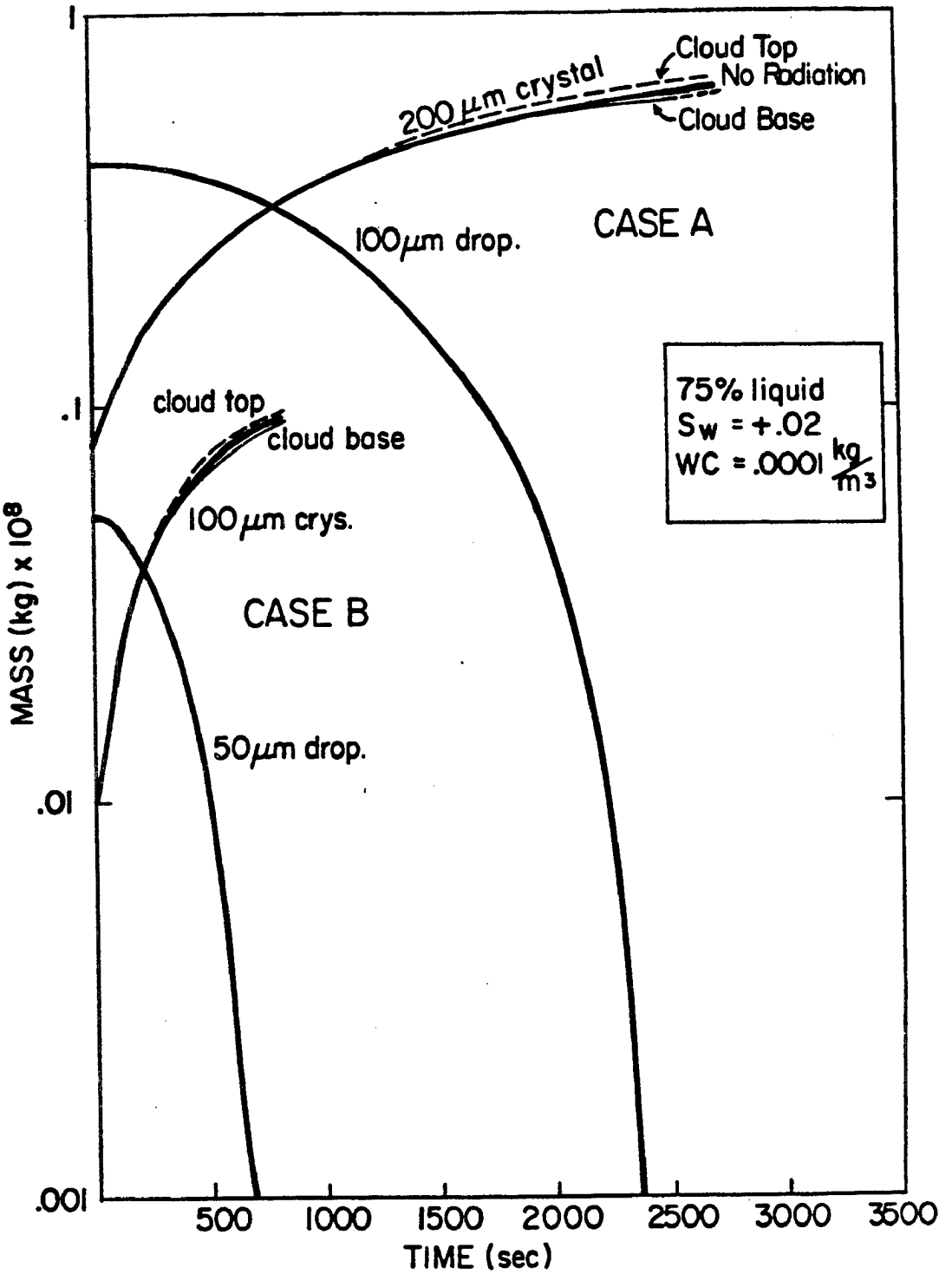

Figure 13. Coexisting mass evolutions; conditions shown.

(case B). Again, the droplets grow only for a few seconds, only to subsequently evaporate (within 11 minutes in this case). The single curves shown for the droplet case represent both radiative and non-radiative conditions.

The coexisting simulations demonstrate that in these situations radiation makes little difference in the mass evolutions. Final masses of crystals and droplet survival times (Table 4) show little variation over the four different radiative conditions. Only the limiting cloud top and cloud base cases are shown. The shortwave, isolated and no radiation simulations lie between the limiting cases.

TABLE 4
DROPLET SURVIVAL TIMES FOR THE VARIOUS CASES

s_w	WC(g/m^3)	% drops	L	r	SURVIVAL TIMES (Seconds) no radiation	cloud top radiation	cloud base radiation
-.15	0.1	75	10	5	10	10	10
-.15	.1	75	20	10	40	40	40
-.15	.1	75	40	25	155	155	155
-.15	.1	75	100	50	560	560	560
-.15	.1	75	200	100	1985	1980	1985
-.15	.1	75	400	200	1 hr	1 hr	1 hr
-.05	.1	75	10	5	10	10	10
-.05	.1	75	20	10	45	45	45
-.05	.1	75	40	25	165	165	165
-.05	.1	75	100	50	635	630	635
-.05	.1	75	200	100	2240	2225	2255
-.05	.1	75	400	200	1 hr	1 hr	1 hr
-.01	.1	75	10	5	10	10	10
-.01	.1	75	20	10	45	45	45
-.01	.1	75	40	25	170	170	175
-.01	.1	75	100	50	660	655	665
-.01	.1	75	200	100	2335	2310	2355
-.01	.1	75	400	200	1 hr	1 hr	1 hr
0.0	.1	75	10	5	10	10	10
0.0	.1	75	20	10	45	45	45
0.0	.1	75	40	25	175	175	175
0.0	.1	75	100	50	665	665	670
0.0	.1	75	200	100	2360	2335	2380
0.0	.1	75	400	200	1 hr	1 hr	1 hr
.01	.1	75	10	5	10	10	10
.01	.1	75	20	10	45	45	45
.01	.1	75	40	25	175	175	175
.01	.1	75	100	50	675	670	675
.01	.1	75	200	100	2380	2355	2400
.01	.1	75	400	200	1 hr	1 hr	1 hr
.02	.1	75	10	5	10	10	10
.02	.1	75	20	10	45	45	45
.02	.1	75	40	25	175	175	175
.02	.1	75	100	50	680	675	685
.02	.1	75	200	100	2405	2375	2425
.02	.1	75	400	200	1 hr	1 hr	1 hr
.01	.1	75	400	10	2330		
.01	.1	75	100	10	245		
.01	.1	75	40	100	1370		
.01	.01	75	200	100	1 hr		
.01	.01	75	100	50	1285		
.01	.01	25	100	50	850		
.01	.1	25	100	50	470		

In these simulations the radiative effects on the water and ice phases act in opposition. For example, in the cloud top case, crystal growth is slightly enhanced by longwave cooling while droplet evaporation is slowed down slightly. The inhibited evaporation of the droplets means less water vapor is available for crystal growth (i.e. s_i tends to be suppressed); thus the enhanced cloud top growth of the crystals is opposed by the effect of cloud top cooling of the droplets. In the cloud base and shortwave cases, evaporation of the droplet is enhanced (i.e. s_i tends to be enhanced) while at the same time growth of crystals is inhibited radiatively. The two effects are again opposed. Thus during the first 20 or 30 minutes of the simulation, while the droplets still have significant mass, the difference between the radiation/no radiation cases is very small. Only later during the portion of the evolutions when the droplet masses are insignificant or nonexistent does the radiation affect the crystal masses appreciably. During this latter portion the radiative effects on the growth rates of the ice crystals are similar to the effect on the single-phase cases with limited moisture available.

Interestingly, the cloud top environment reduces the droplet survival times on the order of less than one minute in the larger-sized coexisting cases. Here, the longwave cooling is affecting the larger crystal more than the small evaporating droplet during the latter portion of the one hour simulation. Initially the opposite is true, since the larger droplet's growth is enhanced more than that of the smaller crystal. After a few minutes, however, the ice supersaturation effect takes over, the crystal grows at the expense of the droplet, and the crystal soon becomes much larger. Hereafter cloud top cooling enhances the crystal growth more than it impedes droplet evaporation, and subsequently the ambient moisture decreases slightly more

rapidly than in the no radiation case. As shown previously, the relative importance of the radiation term increases with particle size.

In the cloud base simulations, droplet survival is enhanced by less than one minute in all cases. In the same way as in the cloud top case, longwave warming is affecting the larger crystal more than the droplet during the latter portion of the simulation, thus reducing the depletion of ambient vapor by the crystals. The net result is that droplets last slightly longer than in the no radiation case. The larger difference in survival time for the large initial sizes is again the result of the increased importance of radiation.

4.3 The roles of hydrometeor size and ambient moisture content in the coexisting situations

Table 4 shows the effect of coexisting sizes and initial moisture supply. The initial droplet size is a major factor in determining how long the droplets can survive with crystals. Droplets of initial 5 μm radius last only 10 seconds with L_i = 10 μm crystals, while the 100 μm droplets survive anywhere from 32 to 40 minutes with 200 μm crystals, depending on the moisture and radiation conditions. In each case the initial droplet and crystal masses are comparable. A special case of 100 μm droplets coexisting with 40 μm crystals at initial s_w = +0.01 is shown in Figure 14 (note the large discrepancy between initial crystal and droplet mass), and the results in droplet survival for only about 22 minutes, though the survival in the corresponding 100 μm droplet/200 μm crystal case is about 39 minutes. This is really not surprising since the crystals are initially so much smaller in mass than the droplets, and thus the crystal concentration is much larger (3.56 cm^{-3} as opposed to 0.0330 cm^{-3} for the larger crystals). Such a high concentration of crystals quickly utilizes most of the water vapor available.

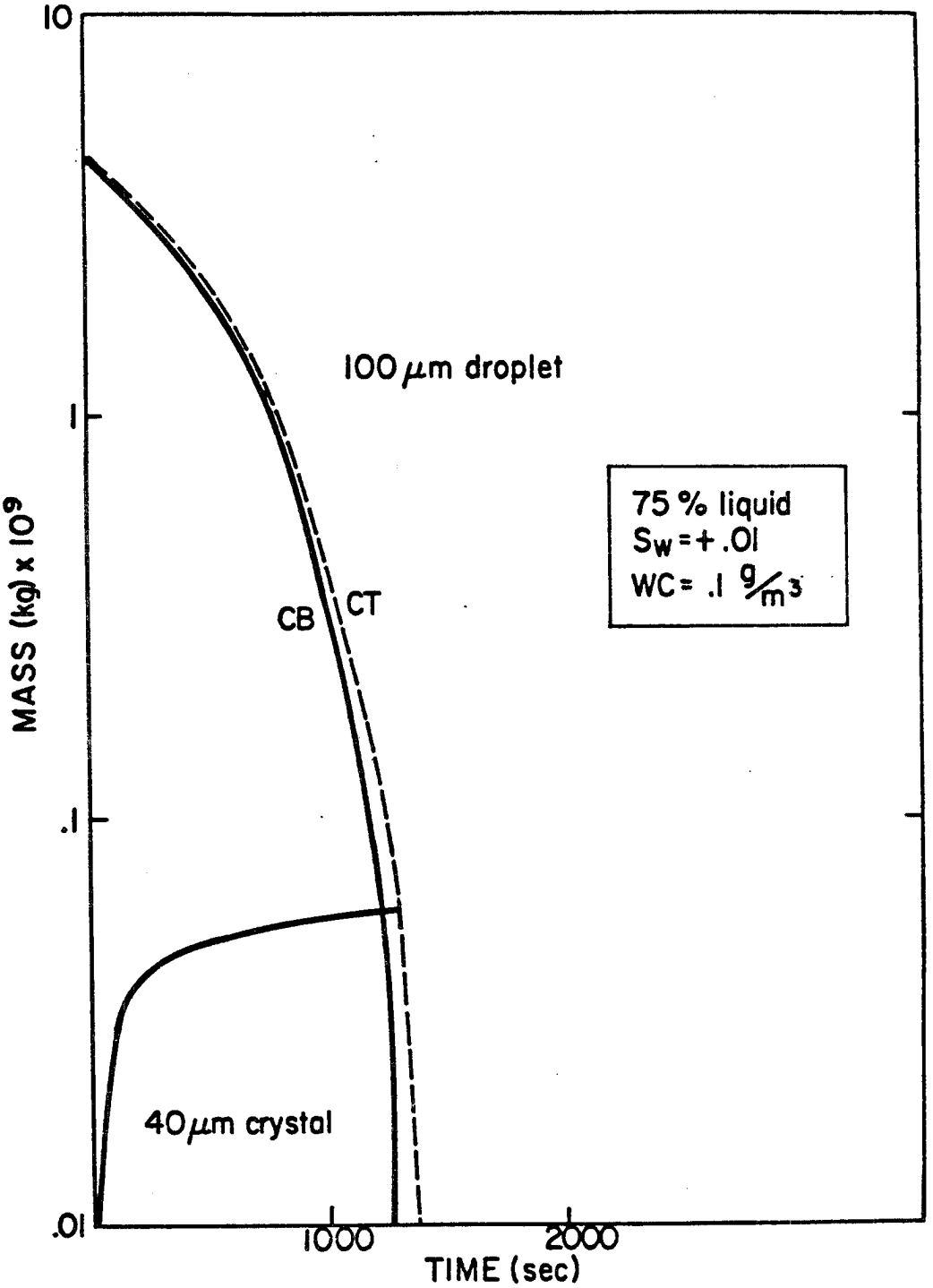

Figure 14. Coexisting mass evolutions; conditions shown.

Thus the high concentration more than offsets the fact that the initial crystal length is much smaller.

Another special case of 10 μm droplets with 100 μm crystals, shown in Figure 15, again at initial s_w = +0.01, results in a few minutes of droplet survival, while in all of the previous cases the maximum 5 or 10 μm droplet survival time is 45 seconds. Again slight enhancement of droplet survival occurs in the cloud base case, and slight decrease at the cloud top (for a clearer graph, the no radiation, shortwave and isolated cases are not shown). Comparison of survival values in Table 4 reveals that droplets of around 10 μm initial size cannot survive for any appreciable time with comparably-sized crystals, but their survival is enhanced when the coexisting crystals are initially much larger (see Figure 15). This result may be explained by the much lower concentration of the larger crystals, and subsequent reduced demand on the available water vapor. Microphysical studies of cirroform clouds (e.g. Heymsfield 1975) have found that larger crystals ($L \geq 100$ μm) exist in much lower concentrations than smaller crystals. The coexistence of a few crystals and a high concentration of small droplets in this study leads to a much longer droplet survival time than in the previous cases. Thus, the 10 μm droplet/100 μm crystal case may apply to actual clouds.

Ambient moisture supply is not important in the coexisting cases of small droplets and small crystals, as shown in Table 4. Even in the 40 μm crystal/25 μm droplet situation, the survival time is about 2 minutes regardless of the initial supersaturation ratio. In the larger hydrometeor (100 μm droplet/200 μm crystal) coexistence cases, the moisture supply has some influence. For example, an increase in initial water supersaturation from -15% to +2% increases droplet survival times by 2 to 7 minutes, while the average survival time is 35 minutes. This difference is fairly small

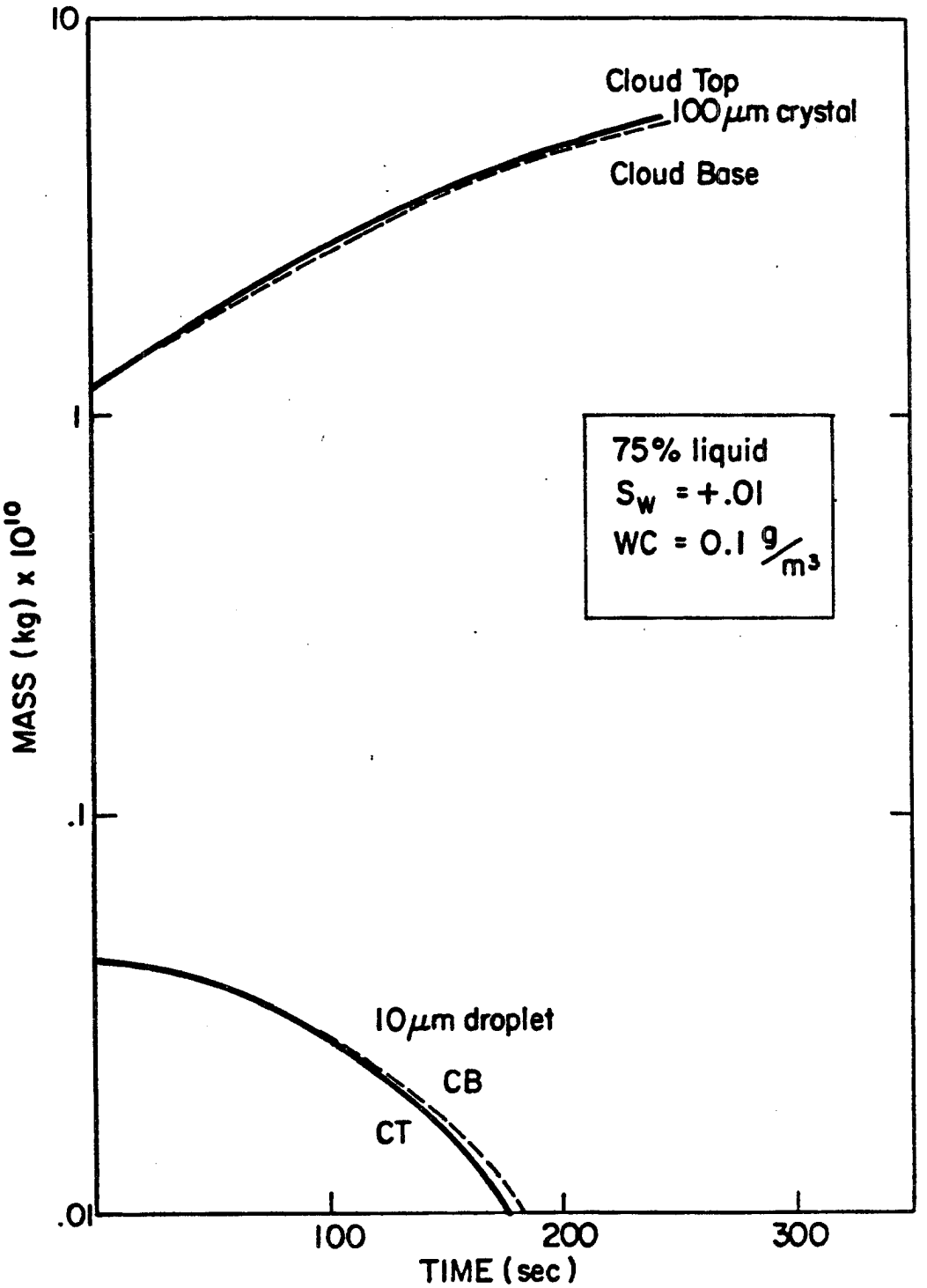

Figure 15. Coexisting mass evolutions; conditions shown.

considering the direct dependence of mass growth rate on ambient vapor density (see equations (1) and (6)). Once again the effects of varying moisture on the ice and water phases are cancelling to some degree. An increase in ambient moisture enhances crystal growth but impedes droplet evaporation. Thus less moisture from droplet evaporation is available to the crystal for growth (i.e. the supersaturation ratio s_i is suppressed). These opposing effects reduce the effect of ambient moisture when the coexisting droplets and crystals are comparable in mass; this is true especially for the smaller hydrometeor coexisting situations, when growth rates are more significant compared with hydrometeor mass. The ambient moisture effects are less significant here than for the single-phase cases.

Similarly, a decrease in environmental vapor density impedes crystal growth but at the same time enhances droplet evaporation, which in turn supplies more vapor for crystal growth (i.e. enhances s_i). The two effects are again approximately cancelling whenever the droplets and crystals are comparable in mass. In the larger hydrometeor cases, the crystal mass and growth rate are large enough to reduce the importance of the limited moisture coming from the shrinking droplets during the latter portion of the one hour simulation, when the droplet size is becoming insignificant. Here, increased initial ambient vapor density begins to make some difference, but still only a few minutes. The moisture effects are opposing whenever the droplets are evaporating while the crystals are growing, and this situation characterizes the vast majority of each simulation.

4.4 The role of hydrometeor concentration in the coexisting cases

By varying the initial IWC plus LWC (total WC), one can examine the effect of droplet and crystal concentrations on the coexisting mass evolutions. This effect already has been discussed briefly. It can be

dramatic, as shown in Figure 16. Figure 16 illustrates a 100 μm droplet/200 μm crystal situation with 75% liquid water, initial s_w = +0.01 and total WC = 0.01 g/m^3. Upon comparison with Table 4 (same size; WC = 0.1 g/m^3) it is evident that the droplet survival is enhanced from about 40 minutes to over 60 minutes, and total crystal growth is also enhanced drastically. For the 200 μm crystal/100 μm droplet case, the survival time has doubled with the tenfold decrease in total WC. Final crystal size is again much larger. In these reduced WC simulations, much more water vapor is available to each hydrometeor due to the reduced concentrations. Thus the change in environmental vapor density is much slower; droplet evaporation is slower and crystal growth is enhanced. The prescribed crystal concentration is critical to the survival times of the droplets. The crystal concentration is more important than the droplet concentration because of the relatively large growth rates of the crystals during all of the simulations. Thus the ambient vapor density (and subsequently the hydrometeor growth rates) are most sensitive to the number density of crystals present.

For some simulations the initial fraction of liquid water was reduced from 75 to 25% to investigate the effect of this ratio on the mass evolutions. As shown in the final two simulations of Table 4 (100 μm crystals/50 μm droplets), droplet survival is impeded significantly with this change; it decreases by several minutes when compared to the previous simulations. The resulting multitude of crystals in these 75% ice cases utilize the available vapor much more quickly than in the previous 25% ice cases. Additional crystals are starting out with a much larger growth rate than the coexisting droplets, as they were in the previous simulations, but in this case there are three times as many crystals to utilize the available water vapor. As stated

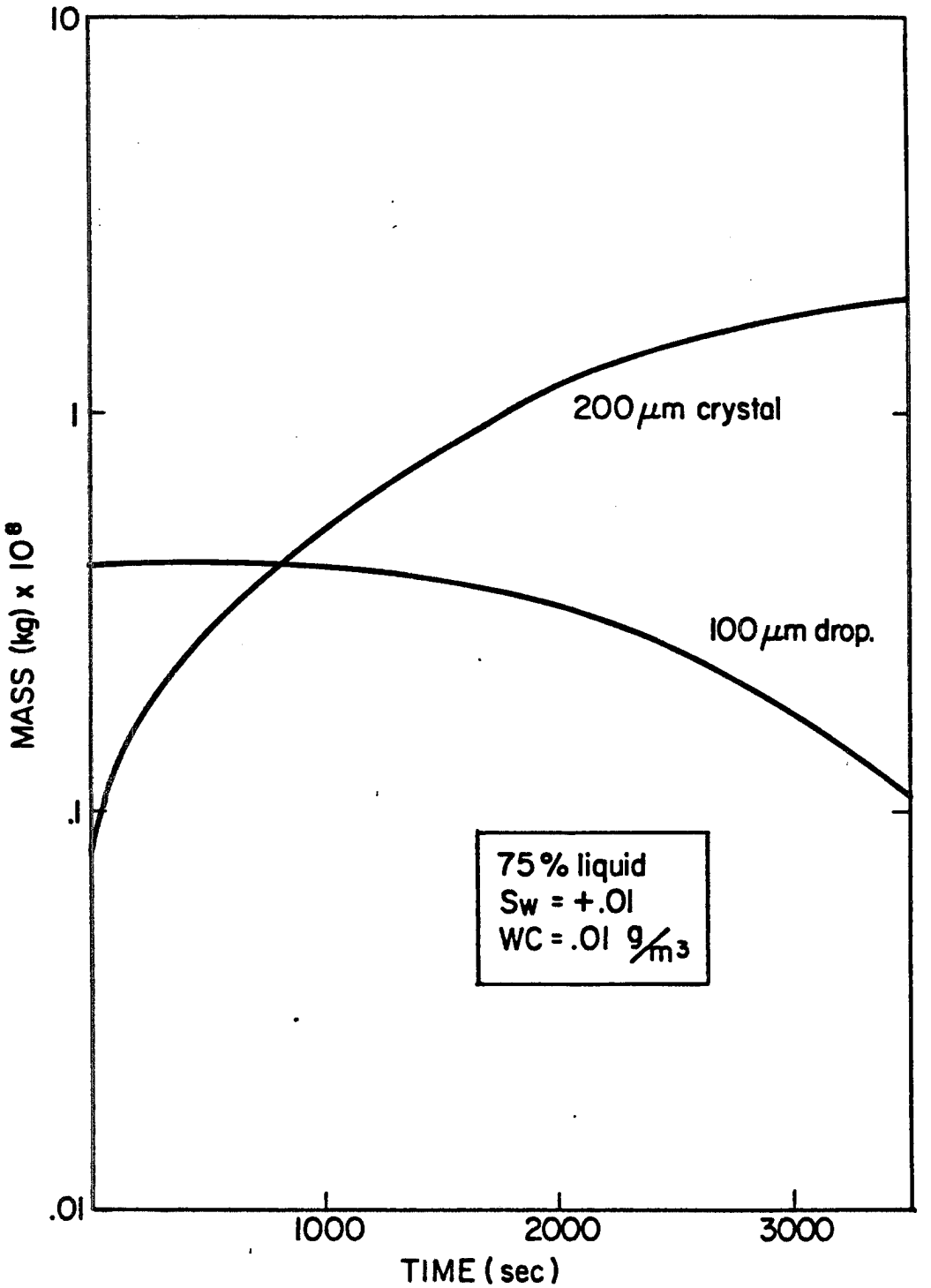

Figure 16. Coexisting mass evolutions; conditions shown.

previously, the ambient vapor density is very sensitive to the number of crystals present.

The results shown in Table 4 demonstrate that droplets of initial radii of less than 200 μm or less cannot coexist with comparably sized crystals for time periods longer than about 40 minutes in regions of high total WC. The crystals promptly dominate the utilization of the available water vapor for growth whether the environment is subsaturated or supersaturated with respect to water. This domination leads quickly to accelerating droplet evaporation until they completely evaporate. The larger cloud droplets of this investigation, say 200 μm in radius, can survive for more than one hour with comparably sized crystals. Droplets can be more persistent only if the concentration of the coexisting crystals is much smaller, e.g. 0.03 cm^{-3}. Due to the lack of microphysical measurements of the typical coexisting sizes in cirroform clouds, it is not clear whether the latter situation is realistic, although larger crystals do tend to exhibit much smaller concentrations in aircraft measurements.

Radiation does not significantly enhance or reduce the droplet survival times. As discussed in Section 4.2, the radiative effects on the two phases cancel to some degree, thus reducing the radiative impact. There is some evidence (Table 4) of slight enhancement of droplet survival times in the maximum radiative warming case at cloud base. Again, the opposing effects on the two phases reduces this change. In these situations, survival time can be enhanced by up to one minute in the larger hydrometeor cases. In the special cases of larger droplets (e.g. 100 μm drops with 40 μm crystals), the effect on survival times is reversed, with a slight decrease of survival time at cloud base, but it is still not very significant. Overall, the cancelling effect between the two phases appears to minimize the radiative impact.

4.5 Simulations of mass evolutions of falling ice crystals

This portion of the modeling investigation determines the radiative influences on the diffusional mass evolutions of columnar ice crystals during their descent through a moist cirrus cloud layer into a relatively dry sub-cloud region. The modeling methods used for these simulations were described in detail in Section 2. Using a parameterized fall velocity, the crystal starts out at cloud top, falls through the 0.5 km moist cloud region, and continues its descent below the cloud until it evaporates. During the fall the crystal encounters the moisture, temperature, and radiative conditions shown in Figure 17. Environmental vapor density is held constant in the two layers.

Figure 18 illustrates the mass evolutions with and without longwave radiative conditions for initial crystal length of 100 μm. Table 5 lists the fall distances (initial height = 7.9 km) and survival times of the crystals for all simulations:

TABLE 5

CRYSTAL SURVIVAL TIMES AND FALL DISTANCES

	fall distance (m)		survival time (sec)	
initial length (μm)	no radiation	radiation	no radiation	radiation
10	657	654	2897	2848
20	657	654	2860	2812
40	658	655	2771	2724
100	667	664	2434	2396
200	746	741	2065	2041
400	1249	1236	2399	2380

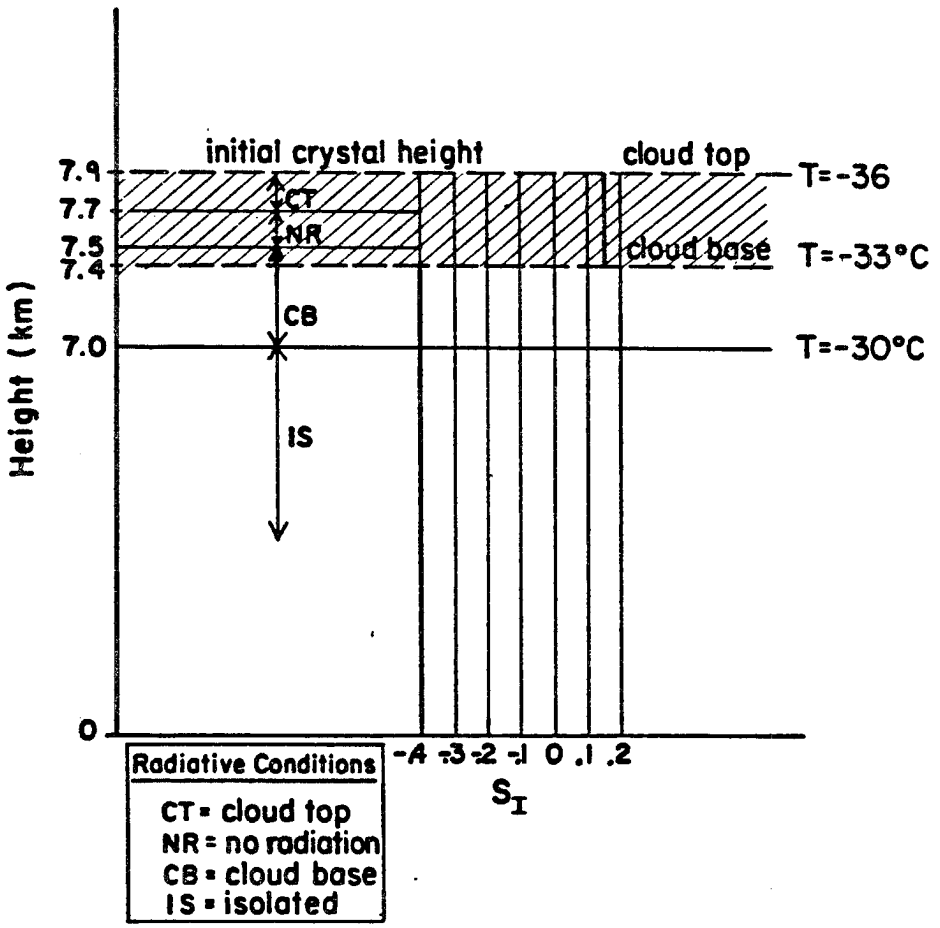

Figure 17. Radiation, moisture and temperature profiles for the falling ice crystal simulations.

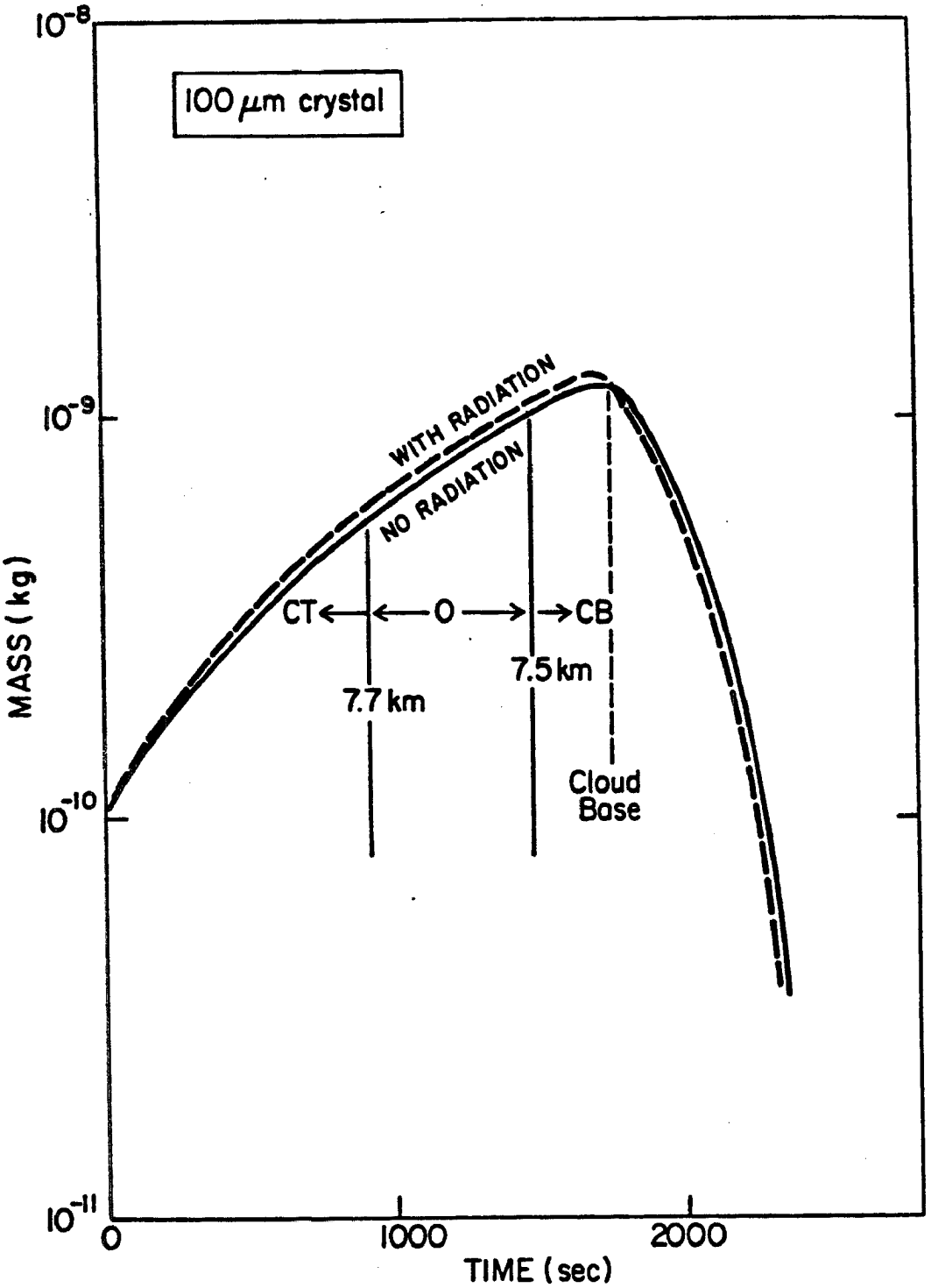

Figure 18. Mass evolutions of falling ice crystal.

The crystals grow rapidly in the cloud and evaporate very quickly once they reach the sub-cloud region. The effect of radiation on the evolutions is insignificant. In all cases cloud-top cooling initially increases the crystal mass growth rate slightly (compared to the no radiation case) until it reaches cloud base, where the radiative effect reverses and cloud-base warming induces additional evaporation as the crystal descends below cloud base. While well inside the cloud layer, the radiation/no radiation growth rates have equal values, since in this region the crystal is assumed to be in radiative equilibrium. The radiative effects here agree with the results of the single-phase simulations discussed previously in that the radiative importance is diminished when the environment is subsaturated or supersaturated by more than a few percent.

Longwave radiation only slightly reduces the survival distance of the crystals. In the smaller crystal simulations, the crystals evaporate so quickly that they never fall into the sub-cloud region, where the crystals would have experienced isolated longwave conditions (near radiative equilibrium; $H \leq 7.0$ km). Thus, they are experiencing cloud-base warming throughout the latter portion of their fall. The 400 μm crystal does fall well below 7.0 km, so it is radiatively isolated during the latter portion of its descent. In all cases, once cloud base is reached the longwave warming quickly enhances the crystal evaporation enough to more than offset the enhanced cloud-top growth. The result is that in all cases longwave radiation slightly reduces the survival distance and survival time; the change ranges from 3 meters for the smallest crystal to only 13 meters for the largest.

V. CONCLUSIONS

A model has been developed and described to investigate radiative-microphysical interactions among hydrometeors in cirroform clouds. This model calculates the diffusional mass evolutions of droplets and ice crystals in a one-phase situation and in a coexisting situation, with various environmental moisture, radiative, and microphysical conditions typically found in cirrus clouds. Coexisting simulations are the simultaneous mass evolutions of ice crystals and droplets in the same cirroform environment. The diffusional mass evolutions of falling ice crystals with and without longwave radiative effects are also calculated.

Detailed examinations of the mass evolutions leads to several pertinent conclusions:

1. Radiative effects on the one-phase simulations are most significant when the environmental water or ice saturation ratio is within 1% of saturation. At slight supersaturation, typical longwave warming or solar absorption can induce slight crystal and droplet evaporation. At slight subsaturation, longwave radiative cooling can induce slight crystal growth and also can reduce diffusional droplet evaporation to near zero.

2. Small liquid water droplets situated with comparably sized ice crystals are not in a stable situation. Regardless of the ambient moisture and radiative conditions, the crystals grow rapidly at the expense of the droplets.

3. Droplet survival times in the coexisting simulations were very sensitive to the crystal concentration. Reduction of crystal concentration by a factor of 10 or more led to enhancement of survival time by several minutes.

4. The minor impact of radiation and moisture conditions on the coexisting mass evolutions is a result of the opposing nature of the effects of these two

properties on the growth rates of the two phases. Radiation and moisture simultaneously have one effect on the growth rate of the droplet and the opposite effect on that of the ice crystal. The net result is that the effects of radiation and moisture in the coexisting simulations are much smaller than in the single-phase simulations.

5. The longwave radiative influences on the diffusional mass evolutions of ice crystals falling through and below a moist cloud layer are insignificant even for large (L = 400 μm) ice crystals. Though large crystals can fall more than 0.5 km further than very small crystals, the fall distances are not significantly affected by longwave radiation.

Based on this study, the expected survival times of cirroform droplets located in close proximity to crystals is less than one hour for cases of high total WC. The vapor pressure difference between ice and water dominates the entire mass evolutions of the hydrometeors. Radiation and ambient moisture effects approximately cancel between the two phases, so droplet enhancement via these two processes is rendered insignificant. In a few extreme cases of droplets coexisting with a low concentration of ice crystals the survival time can be somewhat higher, but such a microphysical situation in cirrus clouds may not be realistic.

VI. REFERENCES

Curran, R. J. and Wu, M.-L. C., 1982: "Skylab near-infrared observations of clouds indicating supercooled liquid water droplets." J. Atmos. Sci., 39, 635-647.

Derrick, W. and Grossman, S., 1981: Elementary differential equations with applications. 2nd ed. Addison-Wesley, p. 296.

Fletcher, R. D. and Sartor, D., 1951: "The Cirrus Forecasting Problem." AWS Tech. Rept. No. 105-81, 11 pp.

Griffith, K. T., Cox, S. K. and Knollenberg, R. G., 1980: "Infrared radiative properties of tropical cirrus clouds inferred from aircraft measurements." J. Atmos. Sci., 37, 1077-1087.

Hall/Pruppacher, 1976: "The survival of ice particles falling from cirrus clouds in subsaturated air." J. Atmos. Sci., 33, 1995.

Heymsfield, A. J., 1975: "Cirrus uncinus generating cells and the evolution of cirroform clouds. Part I: Aircraft observations of the growth of the ice phase." J. Atmos. Sci., 32, 799-808.

Heymsfield, A. J., 1972: "Ice crystal terminal velocities." J. Atmos. Sci., 34, 367-381.

Heymsfield, A. J. and Knollenberg, R. G., 1972: "Properties of Cirrus Generating Cells." J. Atmos. Sci., 29, 1358-1366.

Heymsfield, A. J. and Platt, C. M. R., 1984: "A parameterization of the particle size spectrum of ice clouds in terms of the ambient temperature and the ice water content." J. Atmos. Sci., 41, 846.

Irvine, W. M., and Pollack, J. B., 1968: " Infrared optical properties of water and ice spheres." Icarus, 8, 324-360.

Liou, K.-N., 1980: An introduction to atmospheric radiation. Academic Press, 392 pp.

Pruppacher/Klett, 1978: Microphysics of Clouds and Precipitation D. Reidel Publishing Co., 714 pp.

Ramaswamy, V. and Detwiler, A., 1985: "Interdependence of Radiation and Microphysics in Cirrus Clouds." Advanced Study Program, National Center for Atmospheric Research, 49 pp.

Rogers, R. R., 1979: A Short Course in Cloud Physics. 2nd ed., Pergamon Press, 235 pp.

Sassen, K., Liou, K.-N., Kinne, S. and Griffin, M., 1985: "Highly supercooled cirrus cloud water: confirmation and climatic implications." Science, Jan. 25, 1985, 410-413.

Smith, E., and Vonder Haar, T., 1980: "The development of a multispectral radiative signature technique for estimation of rainfall from satellites." CONTRACT NA-80-SAC-00246, Monthly Progress Report No. 4, Colorado State University.

Starr, D. O'C. and S. K. Cox, 1985: "Cirrus Clouds, Part 1: A Cirrus Cloud Model." J. Atmos. Sci., 42, 2663-2681.

Starr, D. O'C. and S. K. Cox, 1985: "Cirrus Clouds, Part 2: Numerical Experiments on the Formation and Maintenance of Cirrus." J. Atmos. Sci., 42, 2682-2694.

Stephens, G. L., 1983: "The influence of radiative transfer on the mass and heat budgets of ice crystals falling in the atmosphere." J. of Atmos. Sci., 40, 1729.

Varley, D. J., 1978: "Cirrus particle distribution study, Part I." AFGL-TR-78-0192, 77 pp.

Varley, D. J. and Brooks, D. M., "Cirrus particle distribution study, Part II." AFGL-TR-78-0248, 108 pp.

Varley, D. J., 1978: "Cirrus particle distribution study, Part III." AFGL-TR-78-0305, 67 pp.

Varley, D. J. and Bernes, A. A., 1979: "Cirrus particle distribution study, Part IV." AFGL-TR-79-0134, 91 pp.

Wallace, J. M., and Hobbs, P. V., 1977: Atmospheric Science: An Introductory Survey. Academic Press, p. 168.

APPENDIX

List of symbols

B = Planck black body function (see equation 25)

C = capacitance for an individual crystal (an effective size factor)

C_{pa} = specific heat of air at constant pressure

D_v = diffusivity of water vapor

D_v' = modified diffusivity of water vapor

$e_{sat,w}$ = saturation vapor pressure with respect to water

$e_{sat,i}$ = saturation vapor pressure with respect to ice

$G(C,\omega)$ = geometric cross section of the hydrometeor normal to the incident radiation

J = incident radiation from surrounding environment

k_a = thermal conductivity of air

k_a' = modified thermal conductivity of air

k_λ = liquid water absorption coefficient

L_e = latent heat of evaporation

L_s = latent heat of sublimation

m = mass of droplet or crystal

N_{ice} = number concentration of ice crystals in cloud

N_{water} = number concentration of droplets in cloud

p = atmospheric pressure

p_o = reference pressure

Q_1 = thermodynamic function inversely proportional to temperature

List of symbols (continued)

Q_2 = thermodynamic function proportional to ambient air density

Q_R = total radiative power received by a hydrometeor

Q_{abs} = particle efficiency factor for absorption

Q_{ext} = particle efficiency factor for extinction

Q_{sct} = particle efficiency factor for scattering

r = radius of droplet

R_a = gas constant for dry air

R_v = gas constant for water vapor

S = solar constant

s = saturation ratio

s_w = supersaturation ratio with respect to water

s_i = supersaturation ratio with respect ice

t = time

T = ambient temperature

T_{avg} = mean temperature between cloud base and ground

T_g = temperature of ground

T_s = temperature at droplet surface

T_o = reference temperature

x = size parameter of the hydrometeors

z = height

α_c = condensation coefficient

α_t = thermal accommodation coefficient

Δ_t = thermal jump distance

Δ_v = vapor jump length

Δt = model time step

E = R_a/R_v

List of symbols (continued)

ε_1 = emissivity of clear atmosphere between cloud base and ground

κ_{abs} = particle absorption efficiency

K = wavelength of radiation

ρ = density of dry air

$\rho_v(T)$ = ambient vapor density

$\rho_{s,w}(T_s)$ = saturation vapor density at droplet surface

$Q_{s,i}(T_s)$ = saturation vapor density at crystal surface

τ = transmissivity of clear atmosphere between cloud base and ground

χ = mass of condensate / unit mass of air

ω = solid angle

ω_λ = single-scattering albedo